Atmos. Chem. Phys. Discuss., https://doi.org/10.5194/acp-2018-412
Manuscript under review for journal Atmos. Chem. Phys.
Discussion started: 9 July 2018

Atmospheric Chemistry and Physics Discussions

A comprehensive study of hygroscopic properties of calcium- and magnesium-containing salts: implication for hygroscopicity of mineral dust and sea salt aerosols

Liya Guo,[1,5,a] Wenjun Gu,[1,5,a] Chao Peng,[2,5] Weigang Wang,[2] Yong Jie Li,[3] Taomou Zong,[4] Yujing Tang,[1] Zhijun Wu,[4] Qinhao Lin,[1] Maofa Ge,[2,5,6] Guohua Zhang,[1] Min Hu,[4] Xinhui Bi,[1] Xinming Wang,[1,5,6] Mingjin Tang[1,5,*]

1 State Key Laboratory of Organic Geochemistry and Guangdong Key Laboratory of Environmental Protection and Resources Utilization, Guangzhou Institute of Geochemistry, Chinese Academy of Sciences, Guangzhou 510640, China

2 State Key Laboratory for Structural Chemistry of Unstable and Stable Species, Institute of Chemistry, Chinese Academy of Sciences, Beijing, China

3 Department of Civil and Environmental Engineering, Faculty of Science and Technology, University of Macau, Avenida da Universidade, Taipa, Macau, China

4 State Key Joint Laboratory of Environmental Simulation and Pollution Control, College of Environmental Sciences and Engineering, Peking University, Beijing 100871, China

5 University of Chinese Academy of Sciences, Beijing 100049, China

6 Center for Excellence in Regional Atmospheric Environment, Institute of Urban Environment, Chinese Academy of Sciences, Xiamen 361021, China

[a] These two authors contributed equivalently to this work.

* Correspondence: Mingjin Tang (mingjintang@gig.ac.cn)

Atmos. Chem. Phys. Discuss., https://doi.org/10.5194/acp-2018-412
Manuscript under review for journal Atmos. Chem. Phys.
Discussion started: 9 July 2018

Atmospheric Chemistry and Physics Discussions

Abstract

Calcium- and magnesium-containing salts are important components for mineral dust and sea salt aerosols, but their physicochemical properties are not well understood yet. In this study, the hygroscopic properties of eight Ca- and Mg-containing salts, including $Ca(NO_3)_2{\cdot}4H_2O$, $Mg(NO_3)_2{\cdot}6H_2O$, $MgCl_2{\cdot}6H_2O$, $CaCl_2{\cdot}6H_2O$, $Ca(HCOO)_2$, $Mg(HCOO)_2{\cdot}2H_2O$, $Ca(CH_3COO)_2{\cdot}H_2O$ and $Mg(CH_3COO)_2{\cdot}4H_2O$, were systematically investigated using two complementary techniques. A vapor sorption analyzer was used to measure the change of sample mass with relative humidity (RH) under isotherm conditions, and the deliquescence relative humidities (DRH) for temperature in the range of 5-30 ^oC as well as water-to-solute ratios as a function of RH at 5 and 25 ^oC were reported for these eight compounds. DRH values showed a large variation for these compounds; for example, at 25 ^oC the DRH values were measured to be ~28.5% for $CaCl_2{\cdot}6H_2O$ and >95% for $Ca(HCOO)_2$ and $Mg(HCOO)_2{\cdot}2H_2O$. In addition, a humidity-tandem differential analyzer was used to measure the change in mobility diameter with RH (up to 90%) at room temperature, in order to determine the hygroscopic growth factors of aerosol particles generated by atomizing water solutions of these eight compounds. All the aerosol particles studied in this work, very likely to be amorphous, started to grow at very low RH (as low as 10%) and showed continuous growth with RH. The hygroscopic growth factors at 90% RH were found to range from 1.26±0.04 for $Ca(HCOO_2)_2$ and 1.79±0.03 for $Ca(NO_3)_2$, varying significantly for the eight types of aerosols considered herein. Overall, our work provides a systematical and comprehensive investigation of the hygroscopic properties of these Ca- and Mg-containing salts, largely improving our knowledge in the physicochemical properties of mineral dust and sea salt aerosols.

Atmos. Chem. Phys. Discuss., https://doi.org/10.5194/acp-2018-412
Manuscript under review for journal Atmos. Chem. Phys.
Discussion started: 9 July 2018

Atmospheric Chemistry and Physics Discussions

1 Introduction

Mineral dust, mainly emitted from arid and semi-arid regions with an annual flux of ~2000 Tg, is one of the most abundant types of aerosols in the troposphere (Textor et al., 2006; Ginoux et al., 2012). Mineral dust aerosol affects the climate system directly by scattering and absorbing solar and terrestrial radiation (Formenti et al., 2011; Ridley et al., 2016; Chen et al., 2017) and indirectly by serving as cloud condensation nuclei and ice nucleation particles (Hoose and Moehler, 2012; Creamean et al., 2013; Cziczo et al., 2013; Tang et al., 2016a). In addition, deposition of mineral dust particles is an important source of several nutrient elements (Fe and P, for example) for many ecosystems around the globe, thus having significant impacts on biogeochemical cycles in these regions (Jickells et al., 2005; Mahowald et al., 2009; Mahowald et al., 2011; Zhang et al., 2015).

Mineral dust aerosol has an average lifetime of a few days in the atmosphere and can thus be transported over thousands of kilometers (Textor et al., 2006; Uno et al., 2009). During transport mineral dust particles may undergo heterogeneous reactions with trace gases, impacting the abundance of a number of important reactive trace gases both directly and indirectly (Usher et al., 2003; Crowley et al., 2010; Romanias et al., 2012; Tang et al., 2017). These reactions can also lead to change in chemical composition of mineral dust particles (Usher et al., 2003; Li and Shao, 2009; Li et al., 2010; Tang et al., 2012; Romanias et al., 2016) and thereby modification of their physicochemical and optical properties (Krueger et al., 2003; Vlasenko et al., 2006; Liu et al., 2008b; Sullivan et al., 2009; Tang et al., 2016a; Pan et al., 2017). Mineral dust particles contain substantial amounts of carbonates, including $CaCO_3$ (calcite) and $CaMg(CO_3)_2$ (dolomite) (Nickovic et al., 2012; Formenti et al., 2014; Jeong and Achterberg, 2014; Journet et al., 2014; Scanza et al., 2015). These carbonates are largely insoluble and have very low hygroscopicity

(Sullivan et al., 2009; Tang et al., 2016a); however, their reactions with acidic gases in the troposphere can form Ca- and Mg-containing salts with higher hygroscopicity (Gibson et al., 2006; Liu et al., 2008b; Sullivan et al., 2009; Tang et al., 2016a), such as $Ca(NO_3)_2$ and $Mg(NO_3)_2$. For example, numerous laboratory and field studies have found that due to the formation of $Ca(NO_3)_2$ and $CaCl_2$ from heterogeneous reactions with nitrogen oxides (Goodman et al., 2000; Liu et al., 2008a; Li et al., 2010; Tang et al., 2012; Tan et al., 2016) and HCl (Santschi and Rossi, 2006), solid $CaCO_3$ particles could be converted to aqueous droplets under tropospheric conditions (Krueger et al., 2003; Laskin et al., 2005; Liu et al., 2008b; Shi et al., 2008; Tobo et al., 2010). In addition, $MgCl_2$ is an important component in sea salt (as known as sea spray) aerosol. The presence of $MgCl_2$, in addition to NaCl, can alter the hygroscopicity of sea salt aerosol (Gupta et al., 2015; Zieger et al., 2017).

Nevertheless, hygroscopic properties of $Ca(NO_3)_2$, $Mg(NO_3)_2$, $CaCl_2$ and $MgCl_2$ have not been completely understood, especially in the two following aspects. First, hygroscopic growth factors were only measured by one or two previous studies for $Ca(NO_3)_2$ (Gibson et al., 2006; Jing et al., 2018), $Mg(NO_3)_2$ (Gibson et al., 2006), $CaCl_2$ (Park et al., 2009), and $MgCl_2$ aerosols (Park et al., 2009). Considering the importance of these compounds in the troposphere, additional measurements of their hygroscopic growth are clearly warranted. In addition, tropospheric temperatures range from ~200 to ~300 K; however, the effects of temperature on their phase transitions and hygroscopic growth remain largely unclear (Kelly and Wexler, 2005), due to lack of experimental data below room temperature.

Small carboxylic acids, such as formic and acetic acids, are abundant in the troposphere (Khare et al., 1999), and previous studies suggested that heterogeneous reactions of mineral dust with formic and acetic acids are efficient (Hatch et al., 2007; Prince et al., 2008; Tong et al., 2010;

Ma et al., 2012; Tang et al., 2016b). It was shown that calcium and magnesium acetates were formed in heterogeneous reactions of gaseous acetic acid with MgO and $CaCO_3$ particles, leading to a significant increase in particle hygroscopicity (Ma et al., 2012). However, only a few previous studies explored hygroscopic growth of $Mg(CH_3COO)_2$ (Wang et al., 2005; Pang et al., 2015) and $Ca(CH_3COO)_2$ (Ma et al., 2012). To our knowledge, hygroscopic growth factors of aerosol particles have never been studied for $Ca(HCOO)_2$, $Mg(HCOO)_2$, $Ca(CH_3COO)_2$ and $Mg(CH_3COO)_2$.

To better understand the hygroscopic properties of these Ca- and Mg-containing salts, two complementary techniques were employed in this work to investigate their phase transitions and hygroscopic growth. A vapor sorption analyzer, which measured the sample mass as a function of RH, was used to determine the DRH and solute-to-water ratios for $Ca(NO_3)_2{\cdot}4H_2O$, $Mg(NO_3)_2{\cdot}6H_2O$, $CaCl_2{\cdot}6H_2O$, $MgCl_2{\cdot}6H_2O$, $Ca(HCOO)_2$, $Mg(HCOO)_2{\cdot}2H_2O$, $Ca(CH_3COO)_2{\cdot}H_2O$ and $Mg(CH_3COO)_2{\cdot}4H_2O$ at different temperatures (5-30 ºC). Furthermore, hygroscopic growth factors of $Ca(NO_3)_2$, $Mg(NO_3)_2$, $CaCl_2$, $MgCl_2$, $Ca(HCOO)_2$, $Mg(HCOO)_2$, $Ca(CH_3COO)_2$ and $Mg(CH_3COO)_2$ aerosol particles were determined at room temperature up to 90% RH, using a tandem-differential mobility analyzer. This work would significantly increase our knowledge in the hygroscopicity of these compounds, leading to a better understanding of the physicochemical properties of mineral dust and sea salt aerosols.

2 Experimental section

Hygroscopic growth of Ca- and Mg-containing salts were investigated using two complementary techniques, i.e. a humidity-tandem differential mobility analyzer (H-TDMA) and a vapor sorption analyzer (VSA). Eight salts, all supplied by Aldrich, were investigated in this work, including calcium nitrate tetrahydrate (>99%), magnesium nitrate hexahydrate (99%),

calcium chloride hexahydrate (>99%), magnesium chloride hexahydrate (>99%), calcium formate (>99%), magnesium formate dihydrate (98%), calcium acetate monohydrate (>99%), and magnesium acetate tetrahydrate (99%).

2.1 H-TDMA experiments

H-TDMA measurements were carried out at Institute of Chemistry, Chinese Academy of Sciences, and the experimental setup was detailed in previous work (Lei et al., 2014; Peng et al., 2016). Hygroscopic growth of size-selected aerosol particles was determined by measuring changes in their mobility diameters at different RH. An atomizer (MSP 1500) was used to generate aerosol particles. Solutions used for atomization were prepared using ultrapure water, and their typical concentrations were 0.3-0.4 g L^{-1}. The aerosol flow exiting the atomizer was passed through a Nafion dryer and then a diffusion dryer filled with silica gel to reach a final RH of <5%. The aerosol flow was then delivered through a neutralizer and the first differential mobility analyzer (DMA) to produce quasi-monodisperse aerosol particles with a mobility diameter of 100 nm. After that, the aerosol flow was transferred through a humidification section with a residence time of ~27 s to be humidified to a given RH. After humidification, the size distribution of aerosol particles was measured using the second DMA coupled with a condensation particle counter (TSI 3776). For the second DMA, the aerosol flow and the sheath flow were always maintained at the same RH. The flow rate ratios of the aerosol flow to the sheath flow were set to 1:10 for both DMA.

All the experiments were carried out at 298±1 K, and in each experiment hygroscopic growth of aerosol particles was determined at 12 different RH, i.e. <5, 10, 20, 30, 40, 50, 60, 70, 75, 80, 85, and 90%. Hygroscopic growth of each compound was measured three times, and the performance of the H-TDMA setup was routinely checked by measuring the hygroscopic growth

of 100 nm $(NH_4)_2SO_4$ and NaCl aerosol particles, whose hygroscopic growth factors are well documented.

2.2 VSA experiments

The vapor sorption analyzer (Q5000SA), which measured the mass of a particle sample as a function of RH under isotherm conditions, was manufactured by TA Instruments (New Castle, DE, USA). These experiments were performed at Guangzhou Institute of Geochemistry, Chinese Academy of Sciences, and the instrument and experimental method were described elsewhere (Gu et al., 2017a; Gu et al., 2017b; Jia et al., 2018). Experiments could be conducted in a temperature range of 5-85 ºC with an accuracy of ±0.1 ºC and a RH range of 0-98% with an absolute accuracy of ±1%. The mass measurement had a range of 0-100 mg, and its sensitivity was stated to be <0.1 μg. Initial mass of samples used in an experiment was usually in the range of 0.5-1 mg.

Two different types of experiments were carried out. The mass hygroscopic growth was studied in the first type of experiments: after the sample was dried at <1% RH as a given temperature, RH was increased to 90% stepwise with an increment of 10% per step; after that, RH was set to 0% to dry the sample again. The second type of experiments were conducted to measure DRH values: the sample was first dried at a given temperature, and RH was increased to a value which was at least 5% lower than the expected DRH; RH was then increased stepwise with an increment of 1% until a significant increase in sample mass was observed, and the RH at which the sample mass showed a significant increase was equal to its DRH. At each RH the sample was considered to reach equilibrium with the environment when its mass change was <0.1% within 30 min, and RH was changed to the next value only after the sample mass was stabilized.

Atmos. Chem. Phys. Discuss., https://doi.org/10.5194/acp-2018-412
Manuscript under review for journal Atmos. Chem. Phys.
Discussion started: 9 July 2018

Atmospheric Chemistry and Physics Discussions

3 Results and discussion

3.1 Hygroscopicity of nitrates and chlorides

3.1.1 DRH at different temperature

First we investigated the effect of temperature on the DRH of $Ca(NO_3)_2{\cdot}4H_2O$, $Mg(NO_3)_2{\cdot}6H_2O$ and $MgCl_2{\cdot}6H_2O$, which are the most stable forms of corresponding salts for the temperature range (5-30 ^oC) considered in this work (Kelly and Wexler, 2005). Figure 1a shows the change of RH and normalized sample mass as a function of time in an experiment to measure the DRH of $Mg(NO_3)_2{\cdot}6H_2O$ at 25 ^oC. An abrupt and significant increase in sample mass was observed when RH was increased from 52 to 53%, suggesting that the deliquescence occurred between 52 and 53% RH. Therefore, its DRH was measured to be 52.5±0.5 %.

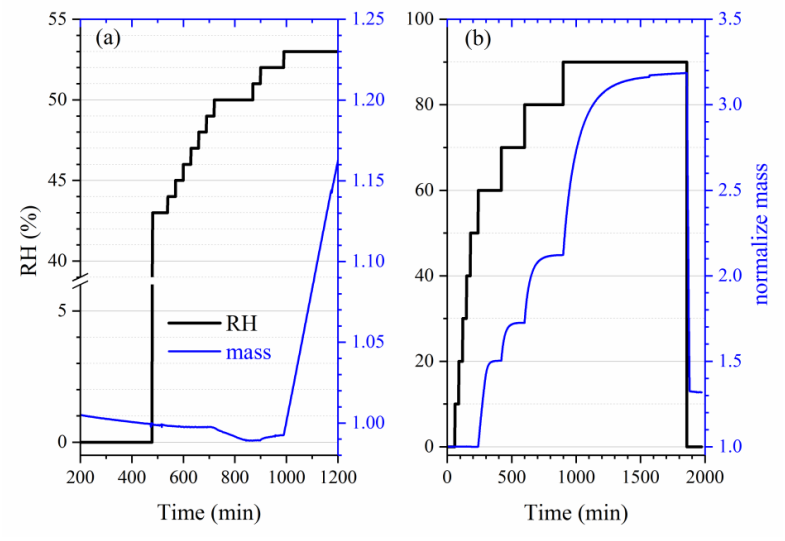

Figure 1. Change of normalized sample mass (blue curve, right *y*-axis) and RH (black curve, left *y*-axis) as a function of time. (a) A typical experiment conducted to measure the DRH; (b) A typical experiment conducted to measure mass hygroscopic growth factors. In the two experiments shown here, $Mg(NO_3)_2{\cdot}6H_2O$ was investigated at 25 ^oC.

Atmos. Chem. Phys. Discuss., https://doi.org/10.5194/acp-2018-412
Manuscript under review for journal Atmos. Chem. Phys.
Discussion started: 9 July 2018

172

173 Table 1 summarizes our measured DRH of $Ca(NO_3)_2{\cdot}4H_2O$, $Mg(NO_3)_2{\cdot}6H_2O$ and
174 $MgCl_2{\cdot}6H_2O$ as a function of temperature (5-30 ^oC). DRH values show a strong dependence on
175 temperature for $Ca(NO_3)_2{\cdot}4H_2O$ (decreasing from 60.5% at 5 ^oC to 46.0% at 30 ^oC) and a weaker
176 temperature dependence for $Mg(NO_3)_2{\cdot}6H_2O$ (decreasing from 57.5% at 5 ^oC to 50.5% at 30 ^oC);
177 in contrast, the DRH values of $MgCl_2{\cdot}6H_2O$ (31.5-32.5 %) exhibit little variation with temperature
178 (5-30 ^oC). Several previous studies have reported the DRH values of $Ca(NO_3)_2{\cdot}4H_2O$,
179 $Mg(NO_3)_2{\cdot}6H_2O$ and $MgCl_2{\cdot}6H_2O$, and their results are compared with our work in the following
180 paragraphs.

181

182 **Table 1.** DRH (in %) of $Ca(NO_3)_2{\cdot}4H_2O$, $Mg(NO_3)_2{\cdot}6H_2O$ and $MgCl_2{\cdot}6H_2O$ measured in this work
183 as a function of temperatures (5-30 ^oC). Solubility data (mol per kg water) compiled by Kelly and
184 Wexler (2005) was used to calculate solubilities in mol per mol water. All the errors (±1 σ) are
185 statistical only.

T (^oC)	$Ca(NO_3)_2{\cdot}4H_2O$	$Mg(NO_3)_2{\cdot}6H_2O$	$MgCl_2{\cdot}6H_2O$
5	60.5±1.0	57.5±1.0	32.5±1.0
10	58.0±1.0	56.5±1.0	32.5±1.0
15	55.5±1.0	54.5±1.0	32.5±1.0
20	52.5±1.0	53.5±1.0	32.5±1.0
25	49.5±1.0	52.5±1.0	31.5±1.0
30	46.0±1.0	50.5±1.0	31.5±1.0
solubility (mol per kg water)	8.4	4.9	5.84
solubility (A, mol per mol water)	0.1512	0.0882	0.1051
$A{\cdot}\Delta H_s/R$ (K)	913±59	427±28	105 [a]
ΔH_s (kJ mol^{-1})	50.2±3.3	40.3±2.6	8.31 [a]

186 [a]: The estimated of $A{\cdot}\Delta H_s/R$ and ΔH_s may have large uncertainties (probably at least a factor of 2) for
187 $MgCl_2{\cdot}6H_2O$. Please refer to Section 3.1.1 for further details.

188

189 **$Ca(NO_3)_2 \cdot 4H_2O$:** RH of air in equilibrium with saturated $Ca(NO_3)_2 \cdot 4H_2O$ solutions, i.e.
190 the DRH values of $Ca(NO_3)_2 \cdot 4H_2O$, were measured to be 55.9, 55.4, 50.5 and 46.7% at 15, 20, 25
191 and 30 °C (Adams and Merz, 1929), and the absolute differences in DRH reported by Adams and
192 Merz (1929) and our work are <3%. The water vapor pressures of saturated $Ca(NO_3)_2 \cdot 4H_2O$
193 solutions were measured to be 0.693, 0.920, 1.253, 1.591 and 1.986 kPa at 10, 15, 20, 25 and 30 °C
194 (Apelblat, 1992), corresponding to DRH values of 56, 54, 54, 50 and 47%, respectively; therefore,
195 DRH measured in our work are in good agreement with those derived from vapor pressure
196 measurements by Apelblat (1992). In another study (Al-Abadleh et al., 2003), RH over the
197 saturated $Ca(NO_3)_2 \cdot 4H_2O$ solution was measured to be 57±5% at room temperature, also in
198 consistence with our work.

199 **$Mg(NO_3)_2 \cdot 6H_2O$:** Water vapor pressures of saturated $Mg(NO_3)_2 \cdot 6H_2O$ solutions were
200 determined to be 0.737, 1.017, 1.390, 1.813 and 2.306 kPa at 10, 15, 20, 25 and 30 °C (Apelblat,
201 1992), giving DRH values of 60, 60, 59, 57 and 54% at corresponding temperatures. The vapor
202 pressure of saturated $Mg(NO_3)_2 \cdot 6H_2O$ solutions at 25 °C were reported to be 1.674 and 1.666 kPa
203 by another two studies (Biggs et al., 1955; Robinson and Stokes, 1959), corresponding to a DRH
204 value of ~53%. In addition, the water activity of the saturated $Mg(NO_3)_2$ solution was measured
205 to be 0.528 at 25 °C (Rard et al., 2004), also suggesting a DRH value of ~53%; similarly, RH over
206 the saturated $Mg(NO_3)_2$ solution was reported to be ~53% at 22-24 °C (Li et al., 2008b). Al-
207 Abadleh and Grassian (2003) investigated the phase transition of the $Mg(NO_3)_2 \cdot 6H_2O$ film, and its
208 DRH was determined to be 49-54% at 23 °C. As shown in Table 1, DRH measured in our work
209 agree very well with those derived from most of previous studies (Biggs et al., 1955; Robinson

and Stokes, 1959; Al-Abadleh and Grassian, 2003; Rard et al., 2004), but are always 3-5% lower than those derived from Apelblat (1992).

$MgCl_2 \cdot 6H_2O$: Kelly and Wexler (2005) calculated DRH of $MgCl_2 \cdot 6H_2O$ from vapor pressures of saturated $MgCl_2 \cdot 6H_2O$ solutions measured by previous work, and found that DRH values were in the range of 33-34% for temperatures at 0-40 °C. In addition, water activity of the saturated $MgCl_2$ solution was reported to be 0.3278 at 25 °C (Rard and Miller, 1981), corresponding to a DRH value of ~33% for $MgCl_2 \cdot 6H_2O$. The DRH values of $MgCl_2 \cdot 6H_2O$ measured in our work, as summarized in Table 1, show excellent agreement with those reported by previous work (Rard and Miller, 1981; Kelly and Wexler, 2005). Phase transition and deliquescence behavior of $CaCl_2 \cdot 6H_2O$ were also investigated in our work and found to be very complex, and the result will be discussed in Section 3.1.3.

The dependence of DRH on temperature can usually be approximated by the Clausius-Clapeyron equation (Zeng et al., 2014; Gu et al., 2017a; Jia et al., 2018):

$$\ln[DRH(T)] = \ln[\mathrm{DRH}(298)] + \frac{A \cdot \Delta H_s}{R}\left(\frac{1}{T} - \frac{1}{298}\right) \quad (1)$$

where T is temperature (K), DRH(T) and DRH(298) are the DRH values at T and 298 K, R is the gas constant (8.314 J mol^{-1} K^{-1}), and ΔH_s is the enthalpy of solution (J mol^{-1}). The dimensionless constant, A, is numerically equal to the water solubility of the salt under investigation in the unit of mol per mol water. Figure 2 shows the dependence of DRH values on temperature for $Ca(NO_3)_2 \cdot 4H_2O$ and $Mg(NO_3)_2 \cdot 6H_2O$, confirming that Eq. (1) can indeed approximate the temperature dependence. The slope, which is equal to $A \cdot \Delta H_s/R$, was determined to be 913±59 K for $Ca(NO_3)_2 \cdot 4H_2O$ and 427±28 K for $Mg(NO_3)_2 \cdot 6H_2O$, and thus ΔH_s was translated to be 50.2±3.3 kJ mol^{-1} for $Ca(NO_3)_2 \cdot 4H_2O$ and 40.3±2.6 kJ mol^{-1} for $Mg(NO_3)_2 \cdot 6H_2O$. The variation of DRH

Atmos. Chem. Phys. Discuss., https://doi.org/10.5194/acp-2018-412
Manuscript under review for journal Atmos. Chem. Phys.
Discussion started: 9 July 2018

values with temperature was very small for $MgCl_2 \cdot 6H_2O$ and thus could not be fitted with Eq. (1). Instead, we used its DRH values at 5 and 30 °C (i.e. 278 and 303 K) to estimate the ΔH_s, using Eq. (2):

$$\frac{A \cdot \Delta H_S}{R} = \frac{\ln[DRH(303)] - \ln[DRH(278)]}{(1/303 - 1/278)} \quad (2)$$

The values of $A \cdot \Delta H_s/R$ and ΔH_s were estimated to be 105 K and 8.31 kJ mol^{-1} for $MgCl_2 \cdot 6H_2O$. It should be emphasized that the estimated ΔH_s value for $MgCl_2 \cdot 6H_2O$ had a large uncertainty (probably a factor of >2) due to the very small dependence of its DRH on temperature.

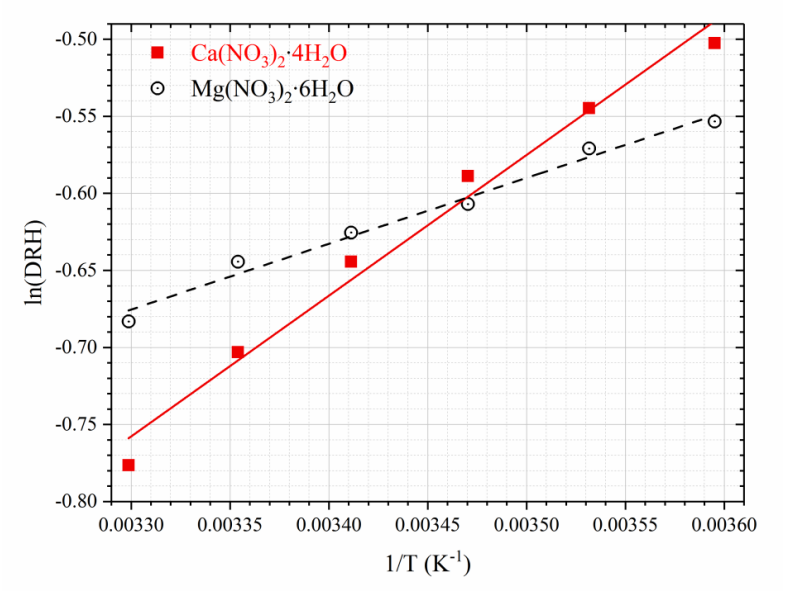

Figure 2. Dependence of DRH values on temperature for $Ca(NO_3)_2 \cdot 4H_2O$ and $Mg(NO_3)_2 \cdot 6H_2O$.

3.1.2 Water-to-solute ratios as a function of RH

The change of sample mass with RH (0-90%) was measured at 5 and 25 °C for $Ca(NO_3)_2 \cdot 4H_2O$, $Mg(NO_3)_2 \cdot 6H_2O$ and $MgCl_2 \cdot 6H_2O$, using the vapor sorption analyzer. The mass change, relative to that at 0% RH, can be used to calculate water-to-solute ratios (WSR, defined in

this work as the molar ratio of H_2O to Ca^{2+} or Mg^{2+}) for deliquesced samples. As summarized in Table 2, decrease in temperature would lead to increase in WSR at 90% RH: WSR were determined to be 28.78±0.20 at 25 °C and 31.80±0.96 at 5 °C for $Ca(NO_3)_2{\cdot}4H_2O$, 36.87±0.23 at 25 °C and 41.40±1.36 at 5 °C for $Mg(NO_3)_2{\cdot}6H_2O$, and 36.26±1.76 at 25 °C and 39.55±2.43 at 5 °C for $MgCl_2{\cdot}6H_2O$, respectively. Several previous studies have measured RH over aqueous $Ca(NO_3)_2$, $Mg(NO_3)_2$, and $MgCl_2$ solutions at given concentrations, and their results are compared with our work, as discussed below.

Table 2. Mass growth factors (m/m_0, defined as the ratio of sample mass at a given RH to that at 0% RH) and water-to-solute ratios (WSR) as a function of RH (0-90%) at 25 and 5 °C for $Ca(NO_3)_2{\cdot}4H_2O$, $Mg(NO_3)_2{\cdot}6H_2O$ and $MgCl_2{\cdot}6H_2O$. WSR were only calculated for RH exceeding the DRH (i.e. when the sample was deliquesced). All the errors (±1 σ) are statistical only.

	$Ca(NO_3)_2{\cdot}4H_2O$, 25 °C		$Ca(NO_3)_2{\cdot}4H_2O$, 5 °C	
RH (%)	m/m_0	WSR	m/m_0	WSR
0	1.000±0.001	--	1.000±0.001	--
10	1.000±0.001	--	1.001±0.001	--
20	1.014±0.005	--	1.005±0.003	--
30	1.016±0.007	--	1.005±0.002	--
40	1.017±0.009	--	1.009±0.003	--
50	1.237±0.006	7.10±0.03	1.032±0.005	4.41±0.02
60	1.363±0.008	8.76±0.05	1.041±0.002	4.54±0.01
70	1.550±0.009	11.22±0.06	1.610±0.010	12.00±0.07
80	1.897±0.012	15.77±0.10	1.979±0.027	16.85±0.23
90	2.889±0.020	28.78±0.20	3.119±0.095	31.80±0.96
	$Mg(NO_3)_2{\cdot}6H_2O$, 25 °C		$Mg(NO_3)_2{\cdot}6H_2O$, 5 °C	
RH (%)	m/m_0	WSR	m/m_0	WSR
0	1.000±0.001	--	1.000±0.001	--
10	1.000±0.001	--	1.000±0.001	--

20	1.000±0.001	--	1.000±0.001	--
30	1.001±0.001	--	1.000±0.001	--
40	1.001±0.001	--	1.000±0.001	--
50	1.000±0.001	--	1.000±0.001	--
60	1.503±0.001	13.15±0.01	1.539±0.003	13.67±0.03
70	1.724±0.001	16.30±0.01	1.773±0.007	16.99±0.07
80	2.121±0.001	21.94±0.01	2.203±0.021	23.11±0.22
90	3.171±0.029	36.87±0.23	3.489±0.114	41.40±1.36

	$MgCl_2 \cdot 6H_2O$, 25 °C		$MgCl_2 \cdot 6H_2O$, 5 °C	
RH (%)	m/m_0	WSR	m/m_0	WSR
0	1.000±0.001	--	1.000±0.001	--
10	1.000±0.001	--	1.000±0.001	--
20	1.000±0.001	--	1.000±0.001	--
30	1.001±0.001	--	1.000±0.001	--
40	1.344±0.057	9.89±0.42	1.327±0.082	9.69±0.60
50	1.489±0.062	11.52±0.48	1.473±0.090	11.34±0.69
60	1.677±0.072	13.65±0.58	1.667±0.100	13.52±0.82
70	1.951±0.084	16.74±0.72	1.950±0.117	16.72±1.00
80	2.433±0.117	22.18±1.06	2.465±0.148	22.54±1.35
90	3.681±0.178	36.26±1.76	3.972±0.244	39.55±2.43

$Ca(NO_3)_2$: Water activities of $Ca(NO_3)_2$ solutions at 25 °C were measured to be 0.904, 0.812 and 0.712 when the concentrations were 2.0 3.5, and 5.0 mol kg^{-1}, respectively (El Guendouzi and Marouani, 2003); in other words, WSR were found to be 11.1, 15.9 and 27.8 at 71.2, 81.2 and 90.4 % RH, respectively. As shown in Table 2, in our work WSR were determined to be 11.22±0.06, 15.77±0.10 and 28.78±0.20 at 70, 80 and 90% RH for $Ca(NO_3)_2$ solutions at the same temperature, suggesting good agreement with El Guendouzi and Marouani (2003).

$Mg(NO_3)_2$: Water activities of $Mg(NO_3)_2$ solutions were reported to be 0.897, 0.812 and 0.702 when the concentrations were 1.6, 2.5 and 3.5 mol kg^{-1} at 25 °C, respectively (Rard et al.,

2004); this means that WSR were equal to 15.9, 22.2 and 34.7 at 70.2, 81.2 and 89.7% RH. Ha and Chan (1999) fitted their measured water activities of $Mg(NO_3)_2$ as a function of molality concentration at 20-24 ^oC with a polynomial equation, and WSR were derived to be 12.93, 16.12, 21.50 and 36.09 at 60, 70, 80, and 90% RH. As shown in Table 2, WSR were measured to be 13.15±0.01, 16.30±0.01, 21.94±0.01 and 36.87±0.23 at 60, 70, 80 and 90% RH for deliquesced $Mg(NO_3)_2$ at 25 ^oC. Therefore, it can be concluded that for WSR of $Mg(NO_3)_2$ solutions at ~25 ^oC, our work shows good agreement with the two previous studies (Ha and Chan, 1999; Rard et al., 2004).

$MgCl_2$: Water activities of $MgCl_2$ solutions were reported to be 0.909, 0.800, 0.692, 0.491 and 0.408 when the concentrations were 1.4, 2.4, 3.2, 4.6 and 5.2 mol kg^{-1} (Rard and Miller, 1981), i.e. WSR were equal to 10.7, 12.1, 17.4, 23.1 and 39.7 at 40.8, 49.1, 69.2, 80.0 and 90.9% RH. In another work (Ha and Chan, 1999), an electrodynamic balance was used to investigate hygroscopic growth of $MgCl_2$ particles at 20-24 ^oC, and the measured molality concentrations of $MgCl_2$ solutions as a function of water activity were fitted by a polynomial equation; it can be derived from Ha and Chen (1999) that WSR were equal to 10.65, 12.34, 14.29, 17.04, 22.24 and 34.78 when RH were 40, 50, 60, 70, 80 and 90%, respectively. WSR measured in our work, as listed in Table 2, are 9.89±0.42, 11.52±0.48, 1.677±0.072, 16.74±0.72, 22.18±1.06 and 36.26±1.76 at 40, 50, 60, 70, 80 and 90% RH. As a result, our work agrees well with the two previous studies (Rard and Miller, 1981; Ha and Chan, 1999) for WSR of $MgCl_2$ solutions as a function of RH at ~25 ^oC.

3.1.3 Phase transition of $CaCl_2 \cdot xH_2O$

The change in sample mass of $CaCl_2 \cdot 6H_2O$ with RH was also investigated at 25 ^oC. As shown in Figure 3, when dried at 0% RH, the sample mass was reduced by 1/3 (from ~1.5 to ~1.0),

289 and it is speculated that $CaCl_2 \cdot 6H_2O$ was converted to $CaCl_2 \cdot 2H_2O$. When RH was increased to
290 10%, no significant increase in sample mass was observed. As RH was further increased to 20%,
291 the sample mass was increased by 48±7%; this may indicate that $CaCl_2 \cdot 2H_2O$ was converted to
292 $CaCl_2 \cdot 6H_2O$, as the ratio of molar mass of $CaCl_2 \cdot 6H_2O$ (219 g mol^{-1}) to $CaCl_2 \cdot 2H_2O$ (147 g mol^{-1})
293 is 1.49, equal to the ratio of sample mass at 20% RH to that at 10% RH. Further increase in RH to
294 30% would lead to additional increase in sample mass, implying the deliquescence of the sample
295 and the formation of an aqueous $CaCl_2$ solution.

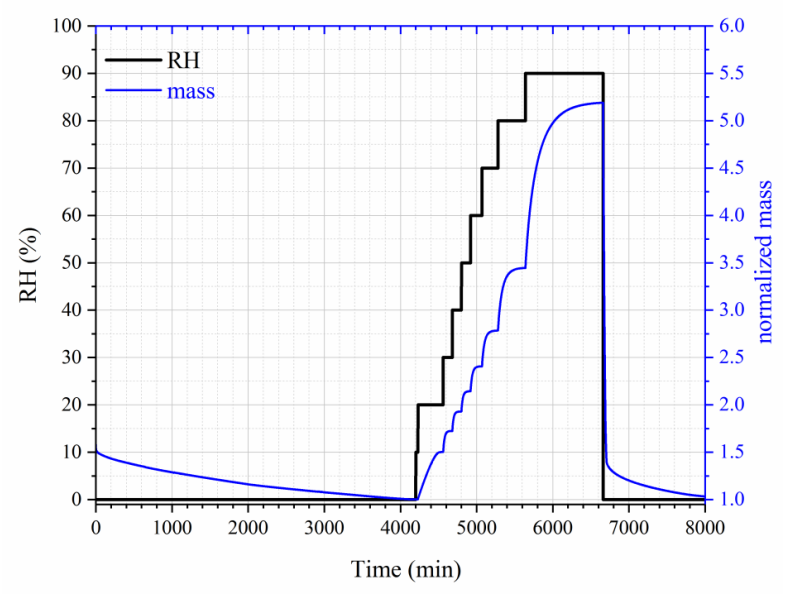

296

297 **Figure 3.** Change of normalized sample mass (blue curve, right *y*-axis) and RH (black curve, left
298 *y*-axis) as a function of time for $CaCl_2 \cdot xH_2O$ at 25 °C.

299

300 Assuming that $CaCl_2 \cdot 6H_2O$ was converted to $CaCl_2 \cdot 2H_2O$ after being dried at 0% RH, we
301 could use the change of sample mass as a function of RH to calculate WSR (defined as molar ratio
302 of H_2O to Ca^{2+}), and the results are listed in Table 3. Please note that we did not calculate WSR at

303 20% RH, since it is speculated that the significant mass increase at 20% RH was caused by the
304 transformation of $CaCl_2 \cdot 2H_2O$ to $CaCl_2 \cdot 6H_2O$, as mentioned above. Water activities of aqueous
305 $CaCl_2$ solutions as a function of molality concentration reported in a previous study (Rard et al.,
306 1977) were used to calculate WSR as a function of RH, and the results are also included in Table
307 3 for comparison. As evident from Table 3, at same/similar RH, WSR measured in our work are
308 in good agreement with those derived from Rard et al. (1977), supporting our assertion that
309 $CaCl_2 \cdot 6H_2O$ was converted to $CaCl_2 \cdot 2H_2O$ after being dried at 0% RH. In fact, theoretical
310 calculations (Kelly and Wexler, 2005) and experimental measurements (Gough et al., 2016) both
311 suggested that when RH is gradually increased, solid-solid phase transition from $CaCl_2 \cdot 2H_2O$ to
312 $CaCl_2 \cdot 6H_2O$ would occur before deliquescence takes place.

313

314 **Table 3.** Mass growth factors (m/m_0, defined as the ratio of sample mass at a given RH to that at
315 0% RH) and water-to-solute ratios (WSR) as a function of RH (0-90%) at 25 °C for $CaCl_2 \cdot xH_2O$.
316 WSR derived from RH over aqueous $CaCl_2$ solutions as a function of concentration (mol kg^{-1}) at
317 25 °C (Rard et al., 1977) are also included for comparison. All the errors (±1 σ) are statistical only.

our work			Rard et al., 1977		
RH (%)	m/m_0	WSR	RH (%)	molality	WSR
0	1.000±0.001	--	--	--	--
10	1.000±0.001	--	--	--	--
20	1.448±0.072	--	--	--	--
30	1.724±0.007	7.97±0.03	31.2	7.0	7.94
40	1.929±0.008	9.64±0.04	39.2	6.0	9.26
50	2.144±0.010	11.40±0.05	49.9	5.0	11.11
60	2.408±0.012	13.55±0.07	--	--	--
70	2.786±0.015	16.64±0.09	70.1	3.4	16.34
80	3.448±0.020	22.05±0.13	79.8	2.6	21.37

90	5.194±0.030	36.30±0.21	89.9	1.6	37.72

318

319 Additional experiments, in which RH was stepwise increased from 0% with an increment
320 of 1% per step, were carried out in attempt to measure the DRH of $CaCl_2 \cdot xH_2O$ at 25 °C. In all of
321 these experiments, $CaCl_2 \cdot 6H_2O$ was always transformed to $CaCl_2 \cdot 2H_2O$ after being dried at 0%
322 RH. In some of these experiments the deliquescence took place at RH of ~28.5%, which is
323 consistent with the DRH of $CaCl_2 \cdot 6H_2O$ reported in the literature (Kelly and Wexler, 2005),
324 suggesting that $CaCl_2 \cdot 2H_2O$ was first transformed to $CaCl_2 \cdot 6H_2O$ prior to deliquescence. However,
325 in some experiments the deliquescence occurred at RH of ~18.5%, corresponding to the DRH of
326 $CaCl_2 \cdot 2H_2O$ reported previously (Kelly and Wexler, 2005), implying that $CaCl_2 \cdot 2H_2O$ was
327 deliquesced without being transformed to $CaCl_2 \cdot 6H_2O$. The dual deliquescence processes, i.e. 1)
328 transformation of $CaCl_2 \cdot 2H_2O$ to $CaCl_2 \cdot 6H_2O$ prior to deliquescence and 2) direct deliquescence
329 of $CaCl_2 \cdot 2H_2O$, were also observed using Raman spectroscopy at low temperatures (223-273 K)
330 (Gough et al., 2016). It seems that the competition of these two mechanisms are both
331 thermodynamically and kinetically dependent. Since phase transitions of $CaCl_2$ are not only
332 important for atmospheric aerosols but may also play a role in the existence of liquid water in some
333 hyperarid environments (Gough et al., 2016), further investigation is being carried out by
334 combining the vapor sorption analyzer technique with vibrational spectroscopy.

335 **3.1.4 Hygroscopic growth of aerosol particles**

336 Hygroscopic growth factors (GF), which were measured using H-TDMA at room
337 temperature, are displayed in Figure 4 for $Ca(NO_3)_2$, $CaCl_2$, $Mg(NO_3)_2$ and $MgCl_2$ aerosols, and
338 the results are also compiled in Table 4. Here GF is defined as the ratio of measured mobility
339 diameters at a given RH to that at dry conditions:

Atmos. Chem. Phys. Discuss., https://doi.org/10.5194/acp-2018-412
Manuscript under review for journal Atmos. Chem. Phys.
Discussion started: 9 July 2018

$$GF = \frac{d}{d_0} \qquad (3)$$

where d_0 and d are the measured mobility diameters at <5% RH and at a given RH, respectively. It was found in our work that all the four types of aerosols exhibit high hygroscopicity, with GF at 90% RH being around 1.7 or larger. In addition, all the four types of aerosol particles, instead of having distinct solid-liquid phase transitions, showed significant hygroscopic growth at very low RH (even as low as 10%), and their GF increased continuously with RH. This phenomenon is due to the fact that these aerosol particles, generated by drying aqueous droplets, were likely in amorphous states. It was also observed in previous work that certain types of particles generated by drying aqueous droplets would be amorphous, such as $Ca(NO_3)_2$ (Tang and Fung, 1997; Gibson et al., 2006; Jing et al., 2018), $Mg(NO_3)_2$ (Zhang et al., 2004; Gibson et al., 2006; Li et al., 2008a), $CaCl_2$ (Park et al., 2009; Tobo et al., 2009) and $MgCl_2$ (Cziczo and Abbatt, 2000; Park et al., 2009).

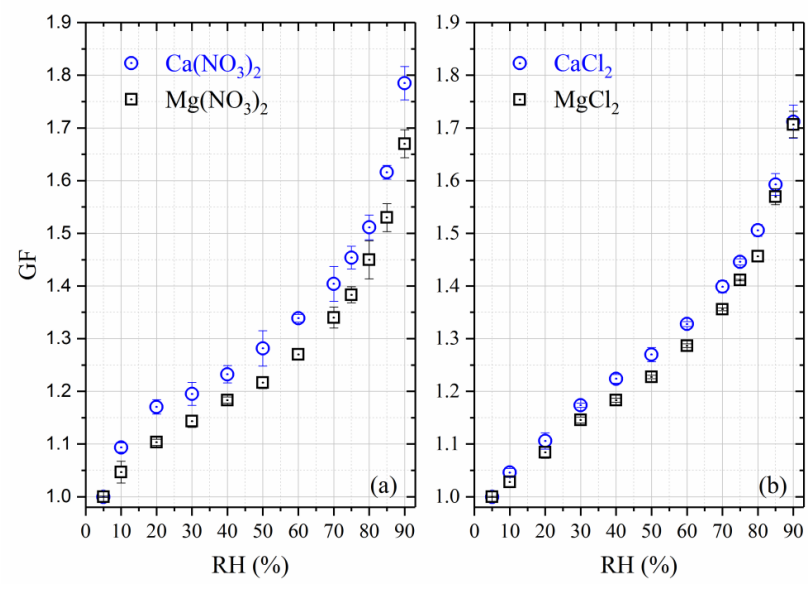

Figure 4. Hygroscopic growth factors (GF) of aerosol particles as a function of RH measured using H-TDMA. (a): $Ca(NO_3)_2$ and $Mg(NO_3)_2$; (b) $CaCl_2$ and $MgCl_2$.

354

355 **$Ca(NO_3)_2$ and $Mg(NO_3)_2$ aerosols:** Two previous studies (Gibson et al., 2006; Jing et al.,
356 2018) employed H-TDMA to examine the hygroscopic growth of $Ca(NO_3)_2$ aerosol particles at
357 room temperature. GF were determined to be 1.51 at 80% RH and ~1.77 at 85% RH by Gibson et
358 al. (2008). It should be pointed out that though the DMA-selected dry particle diameters were 100
359 nm for $Ca(NO_3)_2$ as well as $Mg(NO_3)_2$ aerosols, the dry diameters used by Gibson et al. (2006)
360 were extrapolated to 0% RH using the theoretical growth curve based on the Köhler theory,
361 determined to be were 89 nm for $Ca(NO_3)_2$ and 77 nm for $Mg(NO_3)_2$. The Köhler theory is based
362 on assumption of solution ideality and may not be applicable to highly concentrated aerosol
363 droplets at very low RH (Seinfeld and Pandis, 2006). If the dry diameter selected using the DMA
364 (i.e. 100 nm) was used for calculation instead, GF reported by Gibson et al. (2006) would be ~1.34
365 and ~1.58 at 80 and 85% RH, respectively. In the second study (Jing et al., 2018), GF were
366 determined to 1.56 and 1.89 at 80 and 90% RH. As summarized in Table 4, GF of $Ca(NO_3)_2$ aerosol
367 were measured to be 1.51±0.02, 1.62±0.01 and 1.79±0.03 for 80, 85 and 90% RH in our work,
368 showing reasonably good agreement with the two previous studies (Gibson et al., 2006; Jing et al.,
369 2018).

370

371 **Table 4.** Hygroscopic growth factors (GF) of $Ca(NO_3)_2$, $CaCl_2$, $Mg(NO_3)_2$ and $MgCl_2$ aerosol
372 particles measured using H-TDMA. The given RH values were estimated to have an absolute
373 uncertainty of ±2%.

RH (%)	$Ca(NO_3)_2$	$CaCl_2$	$Mg(NO_3)_2$	$MgCl_2$
5	1.00±0.01	1.00±0.01	1.00±0.01	1.00±0.01
10	1.09±0.01	1.05±0.01	1.05±0.02	1.03±0.01
20	1.17±0.02	1.11±0.02	1.10±0.01	1.08±0.01

30	1.20±0.02	1.17±0.01	1.41±0.01	1.15±0.01
40	1.23±0.02	1.22±0.01	1.18±0.01	1.18±0.01
50	1.28±0.03	1.27±0.01	1.22±0.01	1.23±0.01
60	1.34±0.01	1.33±0.01	1.27±0.01	1.29±0.01
70	1.40±0.03	1.40±0.01	1.34±0.02	1.36±0.01
75	1.45±0.02	1.45±0.01	1.38±0.02	1.41±0.01
80	1.51±0.02	1.51±0.01	1.45±0.04	1.46±0.01
85	1.62±0.01	1.59±0.02	1.53±0.03	1.57±0.02
90	1.79±0.03	1.71±0.03	1.67±0.03	1.71±0.03

To our knowledge, only one previous study investigated the hygroscopic growth of $Mg(NO_3)_2$ aerosol using the H-TDMA (Gibson et al., 2006), and GF was measured to be 1.94±0.02 at 83% RH; as stated above, the theoretical extrapolated diameter (77 nm) at 0% RH, instead of the dry diameter (100 nm) selected using the DMA, were used as the dry diameter to calculate their reported GF (Gibson et al., 2006). If the DMA-selected dry diameter (100 nm) was used in calculation, the GF reported by Gibson et al. (2006) would be ~1.49 at 83% RH. For comparison, in our work GF were determined to be 1.45±0.04 and 1.53±0.03 at 80 and 85% RH, in very good agreement with the results reported by Gibson et al. (2006) if the DMA-selected dry diameter was used in their GF calculation.

$CaCl_2$ and $MgCl_2$ aerosol: Hygroscopic growth of $CaCl_2$ and $MgCl_2$ aerosol particles was explored using a H-TDMA (Park et al., 2009), and as far as we know, this was the only study which reported the H-TDMA measured hygroscopic growth factors of the two aerosols. GF were measured to be around 1.27, 1.38, 1.48 and 1.59 at 60, 75, 80 and 90 % RH for $CaCl_2$ (Park et al., 2009). For comparison, GF were determined to be 1.33±0.01, 1.45±0.01, 1.51±0.01 and 1.71±0.03 at 60, 75, 80 and 90 %, slightly larger than those reported by Park et al. (2009) (though the

390 difference may be insignificant when compared with the relatively large uncertainties associated
391 with their GF which were only presented graphically).

392 At 50, 70, 80, 85 and 90% RH, GF of $MgCl_2$ aerosol were measured to be about 1.17, 1.29,
393 1.47, 1.59 and 1.79 by Park et al. (2009) and 1.23±0.01, 1.36±0.01, 1.46±0.01, 1.57±0.02 and
394 1.71±0.03 in our work, suggesting good agreement between the two studies. Microscopy was used
395 to investigate the hygroscopic growth of micrometer-size $MgCl_2$ particles deposited on substrates
396 (Gupta et al., 2015), and the ratios of 2-D particle areas, relative to that at <5% RH, were measured
397 to be around 1.65, 1.92, 2.02 and 2.28 at 60, 70, 75 and 80% RH, corresponding to diameter-based
398 GF of approximately 1.28, 1.38, 1.42 and 1.51, respectively. GF of $MgCl_2$ aerosol, as shown in
399 Table 4, were determined to be 1.29±0.01, 1.36±0.01, 1.41±0.01 and 1.46±0.01 at 60, 70, 75 and
400 80% RH in our work, agreeing well with those reported by Gupta et al. (2015).

401 **Comparison between growth factors with CCN activities:** GF measured using H-
402 TDMA can be used to calculate the single hygroscopicity parameter, κ_{gf}, using Eq. (4) (Petters and
403 Kreidenweis, 2007; Kreidenweis and Asa-Awuku, 2014; Tang et al., 2016a):

404 $$\kappa_{gf} = (GF^3 - 1)\frac{1-RH}{RH} \qquad (4)$$

405 where GF is the growth factor at a given RH. In our work, GF data at 90% RH were used to derive
406 κ_{gf}, as usually done in many previous studies (Kreidenweis and Asa-Awuku, 2014). The single
407 hygroscopicity parameter, κ_{ccn}, can also be derived from experimental measurements or theoretical
408 calculations of CCN activities (Petters and Kreidenweis, 2007; Kreidenweis and Asa-Awuku,
409 2014), and comparison between κ_{gf} and κ_{ccn} is discussed below.

410 1) For $Ca(NO_3)_2$ aerosol, κ_{ccn} were measured to be 0.44-0.64 by Sullivan et al. (2009) and
411 0.57-0.59 by Tang et al. (2015); in our work GF at 90% RH was measured to be 1.79±0.03, giving

412 κ_{gf} of 0.49-0.56, in good agreement with κ_{ccn} reported by the two previous studies (Sullivan et al.,
413 2009; Tang et al., 2015).

414 2) For $CaCl_2$ aerosol, κ_{ccc} were measured to be 0.46-0.58 by Sullivan et al. (2009) and 0.51-
415 0.54 by Tang et al. (2015); GF at 90% RH was determined to be 1.71±0.03 in the present work,
416 giving κ_{gf} of 0.42-0.47, slightly lower than κ_{ccn} values measured previously (Sullivan et al., 2009;
417 Tang et al., 2015).

418 3) To our knowledge, CCN activities of $Mg(NO_3)_2$ and $MgCl_2$ aerosols have not been
419 experimentally explored yet, and κ_{ccn} were predicted to be 0.8 for $Mg(NO_3)_2$, 0.3 for
420 $Mg(NO_3)_2 \cdot 6H_2O$, and ~1 for $MgCl_2$ (Kelly et al., 2007; Kreidenweis and Asa-Awuku, 2014),
421 exhibiting a large variation for the same compound with different hydrate states under dry
422 conditions. In our work, GF were determined to be 1.67±0.03 and 1.71±0.03 for $Mg(NO_3)_2$ and
423 $MgCl_2$ at 90% RH, corresponding to κ_{gf} of 0.38-0.43 for $Mg(NO_3)_2$ and 0.42-0.47 for $MgCl_2$. As
424 discussed in previous work (Kelly et al., 2007; Zieger et al., 2017), the hydration states, which are
425 not entirely clear for $Mg(NO_3)_2$ and $MgCl_2$ aerosol particles under atmospherically relevant
426 conditions, can have large impacts on their hygroscopicity and CCN activities. Therefore,
427 experimental measurements of CCN activities of $Mg(NO_3)_2$ and $MgCl_2$ aerosols are highly desired.

428 ## 3.2 Hygroscopicity of formates and acetates

429 ### 3.2.1 DRH and water-to-solute ratios

430 We measured the mass change of $Ca(HCOO)_2$, $Mg(HCOO)_2 \cdot 2H_2O$ and
431 $Ca(CH_3COO)_2 \cdot H_2O$ samples as a function of RH at 25 °C, and found that the sample mass
432 remained essentially constant for all the three compounds when RH was increased from 0 to 90%.
433 Therefore, a series of experiments in which RH was increased to 95% were conducted, and for
434 each compounds three duplicate experiments were carried out. As shown in Figure 5a, when RH

435 was increased from 0 to 95%, a significant while small increase in sample mass (>3%) was
436 observed for $Ca(HCOO)_2$. The average ratio of sample mass at 95% RH to that at 0% RH, was
437 determined to be for 1.043±0.018 $Ca(HCOO)_2$ and 1.028±0.008 for $Mg(HCOO)_2{\cdot}2H_2O$ (not
438 shown in Figure 5), probably indicating that the DRH values were >95% for both compounds at
439 25 °C.

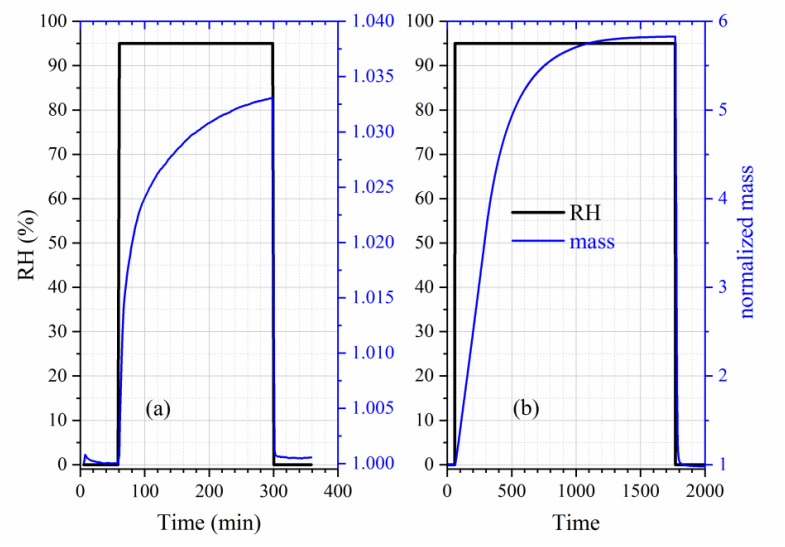

440

441 **Figure 5.** Change of normalized sample mass (blue curve, right *y*-axis) and RH (black curve, left
442 *y*-axis) as a function of time at 25 °C. (a) $Ca(HCOO)_2$; (b) $Ca(CH_3COO)_2{\cdot}H_2O$.

443

444 When RH was increased from 0 to 95%, a very large increase in sample mass (almost by a
445 factor of 6), as shown in Figure 6b, was observed for $Ca(CH_3COO)_2{\cdot}H_2O$. On average, the ratio of
446 sample mass at 95% RH to that at 0% RH was measured to be 5.849±0.064, corresponding to a
447 WSR (defined as the molar ratio of H_2O to Ca^{2+}) of 48.42±0.53 for the aqueous $Ca(CH_3COO)_2$
448 solution at 95% RH. This observation suggested that the deliquescence of $Ca(CH_3COO)_2{\cdot}H_2O$ at
449 25 °C occurred between 90 and 95% RH, and the DRH value of $Ca(CH_3COO)_2{\cdot}H_2O$, measured by

450 further experiments, was determined to be 90.5±1.0 % at 25 °C in our work. The DRH of
451 $Ca(CH_3COO)_2$ and internally mixed $CaCO_3$/$Ca(CH_3COO)_2$ particles were measured to be 85 and
452 88% at 5 °C (Ma et al., 2012), using a modified physisorption analyzer. Since in these two studies
453 the DRH values were measured at different temperatures (25 °C in our work and 5 °C by Ma et
454 al.), the agreement in their reported DRH values can be considered to be quite good for
455 $Ca(CH_3COO)_2$.

456 Table 5 summarizes the ratios of sample mass at a given RH to that at 0% RH for
457 $Mg(CH_3COO)_2{\cdot}4H_2O$ as a function of RH at 25°C. Being different from $Ca(HCOO)_2$,
458 $Mg(HCOO)_2{\cdot}2H_2O$ and $Ca(CH_3COO)_2{\cdot}H_2O$, a large increase in sample mass was observed for
459 $Mg(CH_3COO)_2{\cdot}4H_2O$ when RH was increased from 70 to 80%. This observation suggested that
460 the deliquescence of $Mg(CH_3COO)_2{\cdot}4H_2O$ occurred between 70 and 80% RH. Further
461 experiments were carried out to measure its DRH value, which was determined to be 71.5±1.0%
462 at 25 °C. The RH over the saturated $Mg(CH_3COO_2)_2$ solution at ~23 oC was measured to be 65%
463 (Wang et al., 2005), slightly lower than the DRH value determined in our work.

464

465 **Table 5.** Mass growth factors (m/m_0, defined as the ratios of sample mass at a given RH to that at
466 0% RH) and water-to-solute ratios (WSR) as a function of RH (0-90%) at 25 °C for
467 $Mg(CH_3COO)_2{\cdot}4H_2O$. WSR are only calculated for RH exceeding the DRH (i.e. when the sample
468 was deliquesced). All the errors (±1 σ) are statistical only.

RH (%)	0	10	20	30	40
m/m_0	1.000±0.001	1.012±0.021	1.012 ±0.022	1.013 ±0.022	1.013±0.022
WSR	--	--	--	--	--
RH (%)	50	60	70	80	90
m/m_0	1.014±0.023	1.015±0.025	1.033±0.031	2.029±0.013	3.100±0.021
WSR	--	--	--	16.24±0.11	28.97±0.20

469

470 The ratios of sample mass, relative to that at 0% RH, were measured to be 2.029±0.013
471 and 3.100±0.021 at 80 and 90% RH, corresponding to WSR of 16.24±0.11 at 80% RH and
472 28.97±0.20 at 90% RH for aqueous $Mg(CH_3COO)_2$ solutions. A electrodynamic balance coupled
473 to Raman spectroscopy was employed to study the hygroscopic growth of $Mg(CH_3COO)_2$ at ~23
474 ^oC (Wang et al., 2005), and WSR was determined to be ~15.6 at 80% RH, in good agreement with
475 our work. Ma et al. (2012) found that after heterogeneous reaction with CH_3COOH(g) at 50% RH
476 for 12 h, the hygroscopicity of MgO particles, which was initially rather non-hygroscopic, was
477 substantially increased due to the formation of $Mg(CH_3COO)_2$. The conclusion drawn by Ma et al.
478 (2012) is qualitatively consistent with the results obtained in our work.

479 Table 5 also reveals that a small increase in sample mass (by ~3%, relative to that at 0%
480 RH) was observed for $Mg(CH_3COO)_2{\cdot}4H_2O$ when RH was increased to 70% before its
481 deliquescence occurred. This could be due to the possibility that $Mg(CH_3COO)_2{\cdot}4H_2O$ samples
482 used in our work may contain a small fraction of amorphous $Mg(CH_3COO)_2$, which would take
483 up some amount of water at RH below the DRH of $Mg(CH_3COO)_2{\cdot}4H_2O$ (Wang et al., 2005; Pang
484 et al., 2015).

485 **3.2.2 Hygroscopic growth of aerosol particles**

486 Figure 6 and Table 6 display hygroscopic growth factors of $Ca(HCOO)_2$, $Mg(HCOO)_2$,
487 $Ca(CH_3COO)_2$ and $Mg(CH_3COO)_2$ aerosols, measured in our work using H-TDMA. To the best
488 of our knowledge, this is the first time GF of these four types of aerosols have been reported. For
489 $Mg(HCOO)_2$, aerosol particles showed gradual while small growth for RH up to 30%, and further
490 increase in RH led to significant growth; the average GF of $Mg(HCOO)_2$ aerosol at 90% RH was
491 determined to be 1.69±0.03, similar to those for $Mg(NO_3)_2$ (1.67±0.03) and $MgCl_2$ (1.71±0.03) at

Atmos. Chem. Phys. Discuss., https://doi.org/10.5194/acp-2018-412
Manuscript under review for journal Atmos. Chem. Phys.
Discussion started: 9 July 2018

492 the same RH. For RH up to 85%, $Ca(HCOO)_2$ aerosol particles exhibited gradual and small growth;
493 when RH was increased to 90%, abrupt and large growth was observed, with GF being 1.54±0.02,
494 significantly smaller than that for $Mg(HCOO)_2$ aerosol at the same RH. This is distinctively
495 different from what was observed in VSA experiments, in which the mass of $Ca(HCOO)_2$ and
496 $Mg(HCOO)_2 \cdot 2H_2O$ powdered samples was only increased by <5% when RH was increased from
497 0 to 95%. This difference may be explained by the different states of samples used in these two
498 types of experiments (i. e. crystalline samples in VSA experiments, while likely amorphous aerosol
499 particles in H-TDMA measurements), leading to different hygroscopic behaviors.

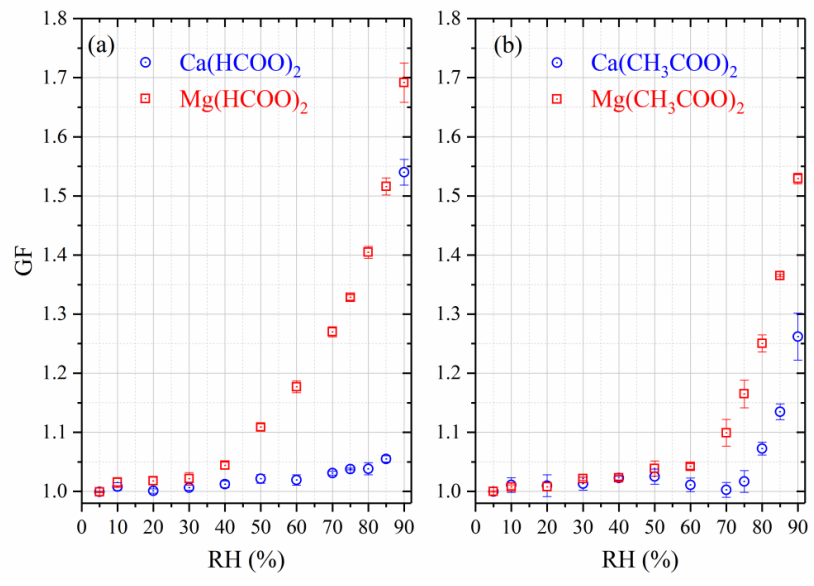

500

501 **Figure 6.** Hygroscopic growth factors (GF) of aerosol particles as a function of RH measured
502 using H-TDMA. (a): $Ca(HCOO)_2$ and $Mg(HCOO)_2$; (b) $Ca(CH_3COO)_2$ and $Mg(CH_3COO)_2$.

503

504 As shown in Figure 6b, gradual and small growth was also observed for $Ca(CH_3COO)_2$
505 and $Mg(CH_3COO)_2$ aerosols at low RH. Fast increase in GF started at about 80% RH for
506 $Ca(CH_3COO)_2$ aerosol, and the GF was determined to be 1.26±0.04 at 90% RH. As discussed in

Section 3.2.1, in VSA experiments no significant increase in sample mass was observed for $Ca(CH_3COO)_2 \cdot H_2O$ when RH was increased from 0 to 90%, being different from H-TDMA results. This difference may again be explained (at least partly) by different states of particles used in these two types of experiments, as mentioned above.

When RH increased from 0 to 70%, small and gradual growth occurred for $Mg(CH_3COO)_2$ aerosol particles, indicating that these particles may contain some amount of amorphous materials. It was also found in previous work (Li et al., 2008a; Li et al., 2008b) that $Mg(NO_3)_2$ particles generated by drying aqueous droplets were amorphous. Figure 6b reveals that further increase in RH led to large increase in growth factors, and this is largely consistent with the occurrence of deliquescence at ~71.5% RH at 25 °C for $Mg(CH_3COO)_2 \cdot 4H_2O$, as mentioned in Section 3.2.1. At 90% RH, GF of $Mg(CH_3COO)_2$ aerosol was determined to be 1.53±0.01, much larger than that for $Ca(CH_3COO)_2$ (1.26±0.04).

At 90% RH, for the four Ca-containing salts considered in our study, nitrate and chloride have very similar GF (1.79±0.03 versus 1.71±0.03), which are large than that of formate (1.54±0.02), and acetate has the smallest GF (1.26±0.04); for comparison, the variation in GF at 90% RH was found to be much smaller (from ~1.53 to ~1.71) for the four Mg-containing salts studied herein.

Table 6. Hygroscopic growth factors of $Ca(HCOO)_2$, $Ca(CH_3COO)_2$, $Mg(HCOO)_2$ and $Mg(CH_3COO)_2$ aerosol particles measured using H-TDMA. The given RH values were estimated to have an absolute uncertainty of ±2%.

RH (%)	$Ca(HCOO)_2$	$Ca(CH_3COO)_2$	$Mg(HCOO)_2$	$Mg(CH_3COO)_2$
5	1.00±0.01	1.00±0.01	1.00±0.01	1.00±0.01
10	1.01±0.01	1.01±0.01	1.02±0.01	1.01±0.01

20	1.01±0.01	1.01±0.02	1.02±0.01	1.01±0.01
30	1.01±0.01	1.01±0.01	1.02±0.01	1.02±0.01
40	1.01±0.01	1.02±0.01	1.04±0.01	1.02±0.01
50	1.02±0.01	1.03±0.01	1.11±0.01	1.04±0.01
60	1.02±0.01	1.01±0.01	1.18±0.01	1.04±0.01
70	1.03±0.01	1.00±0.01	1.27±0.01	1.10±0.02
75	1.04±0.01	1.02±0.02	1.33±0.01	1.16±0.02
80	1.04±0.01	1.07±0.01	1.41±0.01	1.25±0.01
85	1.01±0.01	1.13±0.01	1.52±0.02	1.37±0.01
90	1.54±0.02	1.26±0.04	1.69±0.03	1.53±0.01

According to Eq. (4), GF measured at 90% RH can be used to calculate κ_{gf}, which were determined to be 0.28-0.31 for $Ca(HCOO)_2$, 0.09-0.13 for $Ca(CH_3COO)_2$, 0.40-0.45 for $Mg(HCOO)_2$, and 0.28-0.29 for $Mg(CH_3COO)_2$. A previous study (Tang et al., 2015) investigated the CCN activities of $Ca(HCOO)_2$ and $Ca(CH_3COO)_2$ aerosols and reported their single hygroscopicity parameters (κ_{ccn}), while the CCN activities of $Mg(HCOO)_2$ and $Mg(CH_3COO)_2$ have never been measured before. For $Ca(HCOO)_2$, κ_{ccn} was reported to be 0.47-0.52 (Tang et al., 2015), significantly larger than κ_{gf} (0.28-0.31) determined in our work; for $Ca(CH_3COO)_2$, Tang et al. (2015) reported κ_{ccn} to be in the range of 0.37-0.47, again much larger than κ_{gf} (0.09-0.13) derived from the present work.

As discussed in Section 3.1.4, for $Ca(NO_3)_2$ and $CaCl_2$ aerosols, κ_{gf} derived from H-TDMA experiments in the present work show fairly good agreement with κ_{ccn} derived from CCN activities measured in previous studies (Sullivan et al., 2009; Tang et al., 2015); in contrast, for $Ca(HCOO)_2$ and $Ca(CH_3COO)_2$ aerosols, κ_{gf} derived from our H-TDMA experiments are significantly smaller than κ_{ccn} reported by the previous study (Tang et al., 2015). This is largely caused by the difference in water solubilities of $Ca(NO_3)_2$, $CaCl_2$, $Ca(HCOO)_2$ and $Ca(CH_3COO)_2$. $Ca(NO_3)_2{\cdot}4H_2O$ and $CaCl_2{\cdot}6H_2O$, the solubilities of which are 1983 and 1597 g per kg water at 25 ^oC (Kelly and Wexler,

2005), can be considered to be highly soluble; for comparison, the solubilities were reported to be 166 g per kg water for $Ca(HCOO)_2$ at 25 °C and 347 g per kg water for $Ca(CH_3COO)_2 \cdot 2H_2O$ at 20 °C (Dean, 1973). Due to their limited water solubilities, $Ca(HCOO)_2$ and $Ca(CH_3COO)_2$ aerosol particles may not be fully dissolved when exposed to 90% RH in the H-TDMA experiments but would be dissolved to a larger extent (if not completely) for RH >100% in CCN activity measurements (Petters and Kreidenweis, 2008; Kreidenweis and Asa-Awuku, 2014). Therefore, for $Ca(HCOO)_2$ and $Ca(CH_3COO)_2$ aerosols, κ_{gf} derived from H-TDMA measurements would be smaller than κ_{ccn} derived from CCN activity measurements. In fact, the observation that κ_{gf} appeared to be significantly smaller than κ_{ccn}, largely caused by limited water solubilities of compounds under investigation, has been well documented in the literature for laboratory-generated and ambient aerosol particles (Chang et al., 2007; Prenni et al., 2007; Wex et al., 2009; Good et al., 2010; Massoli et al., 2010).

4. Conclusion and atmospheric implications

Ca- and Mg-containing salts, including nitrates, chlorides, formates and acetates, are important components for mineral dust and sea salt aerosols; however, their hygroscopic properties are not well understood yet. In this work, phase transition and hygroscopic growth of these eight compounds were systematically examined using a vapor sorption analyzer and a humidity-tandem differential mobility analyzer. DRH values decreased from 60.5±1.0% at 5 °C to 46.0±1.0% at 30 °C for $Ca(NO_3)_2 \cdot 4H_2O$ and from 57.5±1.0% at 5 °C to 50.5±1.0% at 30 °C for $Mg(NO_3)_2 \cdot 6H_2O$, both showing negative dependence on temperature, while no significant dependence of DRH (around 31-33%) on temperature (5-30 °C) was observed for $MgCl_2 \cdot 6H_2O$. $CaCl_2 \cdot 6H_2O$, found to deliquesce at ~28.5% RH at 25 °C, exhibited complex phase transition processes in which $CaCl_2 \cdot 2H_2O$, $CaCl_2 \cdot 6H_2O$ and aqueous $CaCl_2$ solutions were involved. Furthermore, DRH values

were determined to be 90.5±1.0% for $Ca(CH_3COO)_2 \cdot H_2O$ and 71.5±1.0% for $Mg(CH_3COO)_2 \cdot 4H_2O$ at 25 °C; for comparison, the sample mass was only increased by <5% for $Ca(HCOO)_2$ and $Mg(HCOO)_2 \cdot 2H_2O$ when RH was increased from 0 to 95%, suggesting that the DRH values of these two compounds were >95%.

We have also measured the change of sample mass as a function of RH up to 90% to derive the water-to-solute ratios (WSR) for deliquesced samples. WSR were determined at 25 and 5 °C for deliquesced $Ca(NO_3)_2 \cdot 4H_2O$, $Mg(NO_3)_2 \cdot 6H_2O$ and $MgCl_2 \cdot 6H_2O$ samples, and at 25 °C for deliquesced $CaCl_2 \cdot 6H_2O$ and $Mg(CH_3COO)_2 \cdot 4H_2O$ samples. We found that compared to that at 0% RH, large increases in sample mass only occurred when RH was increased from 90 to 95% for $Ca(CH_3COO)_2 \cdot H_2O$, and the WSR value was determined to be 5.849±0.064 at 95% RH. Besides, deliquescence was not observed even when RH was increased to 95% for $Ca(HCOO)_2$ and $Mg(HCOO)_2 \cdot 2H_2O$, and the ratios of sample mass at 95% to that at 0% RH, were determined to be for 1.043±0.018 for $Ca(HCOO)_2$ and 1.028±0.008 for $Mg(HCOO)_2 \cdot 2H_2O$. Despite that these compounds are important components for tropospheric aerosols, in general they have not been included in widely used aerosol thermodynamic models, such as E-AIM (Clegg et al., 1998) and ISORROPIA II (Fountoukis and Nenes, 2007). The systematical and comprehensive datasets which we have obtained in this work are highly valuable and can be used to validate thermodynamic models if they are extended to include these compounds.

In addition, hygroscopic growth of aerosol particles was measured at room temperature for these eight compounds. Being different from solid samples for which the onset of deliquescence was evident, aerosol particles were found to grow in a continuous manner since very low RH (as low as 10%), implying that dry aerosol particles of these eight compounds generated from aqueous droplets were amorphous. Hygroscopic growth factors of aerosol particles at 90% RH were

591 determined to be 1.79±0.03 and 1.67±0.03 for $Ca(NO_3)_2$ and $Mg(NO_3)_2$, 1.71±0.03 for both $CaCl_2$
592 and $MgCl_2$, 1.54±0.02 and 1.69±0.03 for $Ca(HCOO)_2$ and $Mg(HCOO)_2$, and 1.26±0.04 and
593 1.53±0.01 for $Ca(HCOO)_2$ and $Mg(HCOO)_2$. GF at 90% show a significant variation (from ~1.26
594 to ~1.79) for the Ca-containing salts investigated here: among them nitrate and chloride have very
595 similar GF (1.79±0.03 versus 1.71±0.03), which are larger than that of formate (1.54±0.02), while
596 acetate has the smallest GF (1.26±0.04). Interestingly, for the four Mg-containing salts considered
597 in this work, the variation in GF at 90 % RH was found to be much smaller (from ~1.53 to ~1.71).

598 GF at 90% RH were used to derive the single hygroscopicity parameters (κ), which were
599 determined to be 0.49-0.56 and 0.38-0.43 for $Ca(NO_3)_2$ and $Mg(NO_3)_2$, 0.42-0.47 for both $CaCl_2$
600 and $MgCl_2$, 0.28-0.31 and 0.40-0.45 for $Ca(HCOO)_2$ and $Mg(HCOO)_2$, and 0.40-0.45 and 0.28-
601 0.29 for $Ca(HCOO)_2$ and $Mg(HCOO)_2$ aerosols, respectively. $Ca(NO_3)_2$ and $CaCl_2$ are very soluble
602 in water, and thus their κ values derived from our H-TDMA experiments are consistent with those
603 reported by previous CCN activity measurements (Sullivan et al., 2009; Tang et al., 2015); on the
604 other hand, due to limited water solubilities, for $Ca(HCOO)_2$ and $Ca(CH_3COO)_2$, κ values derived
605 from our H-TDMA experiments are significantly smaller than those derived from CCN activities
606 measured in a previous study (Tang et al., 2015). Overall, our work would significantly improve
607 our knowledge in the hygroscopic properties of Ca- and Mg-containing salts, and thereby help
608 better understand the physicochemical properties of mineral dust and sea salt aerosols.
609

610 ## Acknowledgement

611 Financial support provided by the National Natural Science Foundation of China
612 (91744204, 91644106 and 41675120), the Chinese Academy of Sciences international
613 collaborative project (132744KYSB20160036) and the special fund of State Key Joint Laboratory

of Environment Simulation and Pollution Control (17K02ESPCP) is acknowledged. Mingjin Tang also would like to thank the CAS Pioneer Hundred Talents program for providing a starting grant. Yujing Tang contributed to this work as an undergraduate intern at Guangzhou Institute of Geochemistry.

References

Adams, J. R., and Merz, A. R.: Hygroscopicity of Fertilizer Materials and Mixtures, Ind. Eng. Chem., 21, 305-307, 1929.

Al-Abadleh, H. A., and Grassian, V. H.: Phase transitions in magnesium nitrate thin films: A transmission FT-IR study of the deliquescence and efflorescence of nitric acid reacted magnesium oxide interfaces, J. Phys. Chem. B, 107, 10829-10839, 2003.

Al-Abadleh, H. A., Krueger, B. J., Ross, J. L., and Grassian, V. H.: Phase transitions in calcium nitrate thin films, Chem. Commun., 2796-2797, 2003.

Apelblat, A.: The vapor pressures of water over saturated solutions of barium chloride, magnesium nitrate, calcium nitrate, potassium carbonate, and zinc sulfate at temperatures from 283 K to 323 K, J. Chem. Thermodyn., 24, 619-626, 1992.

Biggs, A. I., Parton, H. N., and Robinson, R. A.: The Constitution of the Lead Halides in Aqueous Solution, J. Am. Chem. Soc., 77, 5844-5848, 1955.

Chang, R. Y. W., Liu, P. S. K., Leaitch, W. R., and Abbatt, J. P. D.: Comparison between measured and predicted CCN concentrations at Egbert, Ontario: Focus on the organic aerosol fraction at a semi-rural site, Atmos. Environ., 41, 8172-8182, 2007.

Chen, S. Y., Huang, J. P., Kang, L. T., Wang, H., Ma, X. J., He, Y. L., Yuan, T. G., Yang, B., Huang, Z. W., and Zhang, G. L.: Emission, transport, and radiative effects of mineral dust from the Taklimakan and Gobi deserts: comparison of measurements and model results, Atmos. Chem. Phys., 17, 2401-2421, 2017.

Clegg, S. L., Brimblecombe, P., and Wexler, A. S.: Thermodynamic Model of the System H^+–NH_4^+–Na^+–SO_4^{2-}–NO_3^-–Cl^-–H_2O at 298.15 K, J. Phys. Chem. A., 102, 2155-2171, 1998.

Creamean, J. M., Suski, K. J., Rosenfeld, D., Cazorla, A., DeMott, P. J., Sullivan, R. C., White, A. B., Ralph, F. M., Minnis, P., Comstock, J. M., Tomlinson, J. M., and Prather, K. A.: Dust and Biological Aerosols from the Sahara and Asia Influence Precipitation in the Western U.S, Science, 339, 1572-1578, 2013.

Crowley, J. N., Ammann, M., Cox, R. A., Hynes, R. G., Jenkin, M. E., Mellouki, A., Rossi, M. J., Troe, J., and Wallington, T. J.: Evaluated Kinetic and Photochemical Data for Atmospheric Chemistry: Volume V - Heterogeneous Reactions on Solid Substrates, Atmos. Chem. Phys., 10, 9059-9223, 2010.

Cziczo, D. J., and Abbatt, J. P. D.: Infrared observations of the response of NaCl, MgCl2, NH4HSO4, and NH4NO3 aerosols to changes in relative humidity from 298 to 238 K, J. Phys. Chem. A, 104, 2038-2047, 2000.

Cziczo, D. J., Froyd, K. D., Hoose, C., Jensen, E. J., Diao, M., Zondlo, M. A., Smith, J. B., Twohy, C. H., and Murphy, D. M.: Clarifying the Dominant Sources and Mechanisms of Cirrus Cloud Formation, Science, 340, 1320-1324, 2013.

Dean, J. A.: Lange's Handbook on Chemistry (Eleventh Edition), McGraw-Hill, Inc., New York, 1973.

El Guendouzi, M., and Marouani, M.: Water activities and osmotic and activity coefficients of aqueous solutions of nitrates at 25 degrees C by the hygrometric method, J. Solution Chem., 32, 535-546, 2003.

Formenti, P., Rajot, J. L., Desboeufs, K., Saïd, F., Grand, N., Chevaillier, S., and Schmechtig, C.: Airborne observations of mineral dust over western Africa in the summer Monsoon season: spatial and vertical variability of physico-chemical and optical properties, Atmos. Chem. Phys., 11, 6387-6410, 2011.

Formenti, P., Caquineau, S., Desboeufs, K., Klaver, A., Chevaillier, S., Journet, E., and Rajot, J. L.: Mapping the physico-chemical properties of mineral dust in western Africa: mineralogical composition, Atmos. Chem. Phys., 14, 10663-10686, 2014.

Fountoukis, C., and Nenes, A.: ISORROPIA II: a computationally efficient thermodynamic equilibrium model for K^+-Ca^{2+}-Mg^{2+}-NH_4^+-Na^+-SO_4^{2-}-NO_3^--Cl^--H_2O aerosols, Atmos. Chem. Phys., 7, 4639-4659, 2007.

Gibson, E. R., Hudson, P. K., and Grassian, V. H.: Physicochemical properties of nitrate aerosols: Implications for the atmosphere, J. Phys. Chem. A, 110, 11785-11799, 2006.
Ginoux, P., Prospero, J. M., Gill, T. E., Hsu, N. C., and Zhao, M.: Global-scale Attribution of Anthropogenic and Natural Dust Sources and Their Emission Rates Based on MODIS Deep Blue Aerosol Products, Rev. Geophys., 50, RG3005, doi: 3010.1029/2012RG000388, 2012.
Good, N., Topping, D. O., Duplissy, J., Gysel, M., Meyer, N. K., Metzger, A., Turner, S. F., Baltensperger, U., Ristovski, Z., Weingartner, E., Coe, H., and McFiggans, G.: Widening the gap between measurement and modelling of secondary organic aerosol properties?, Atmos. Chem. Phys., 10, 2577-2593, 2010.
Goodman, A. L., Underwood, G. M., and Grassian, V. H.: A Laboratory Study of the Heterogeneous Reaction of Nitric Acid on Calcium Carbonate Particles, J. Geophys. Res.-Atmos., 105, 29053-29064, 2000.
Gough, R. V., Chevrier, V. F., and Tolbert, M. A.: Formation of liquid water at low temperatures via the deliquescence of calcium chloride: Implications for Antarctica and Mars, Planetary and Space Science, 131, 79-87, 2016.
Gu, W. J., Li, Y. J., Tang, M. J., Jia, X. H., Ding, X., Bi, X. H., and Wang, X. M.: Water uptake and hygroscopicity of perchlorates and implications for the existence of liquid water in some hyperarid environments, RSC Adv., 7, 46866-46873, 2017a.
Gu, W. J., Li, Y. J., Zhu, J. X., Jia, X. H., Lin, Q. H., Zhang, G. H., Ding, X., Song, W., Bi, X. H., Wang, X. M., and Tang, M. J.: Investigation of water adsorption and hygroscopicity of atmospherically relevant particles using a commercial vapor sorption analyzer, Atmos. Meas. Tech., 10, 3821-3832, 2017b.
Gupta, D., Eom, H. J., Cho, H. R., and Ro, C. U.: Hygroscopic behavior of NaCl-MgCl2 mixture particles as nascent sea-spray aerosol surrogates and observation of efflorescence during humidification, Atmos. Chem. Phys., 15, 11273-11290, 2015.
Ha, Z., and Chan, C. K.: The Water Activities of MgCl2, Mg(NO3)2, MgSO4, and Their Mixtures, Aerosol Sci. Technol., 31, 154-169, 1999.
Hatch, C. D., Gough, R. V., and Tolbert, M. A.: Heterogeneous Uptake of the C1 to C4 Organic Acids on a Swelling Clay Mineral, Atmos. Chem. Phys., 7, 4445-4458, 2007.
Hoose, C., and Moehler, O.: Heterogeneous ice nucleation on atmospheric aerosols: a review of results from laboratory experiments, Atmos. Chem. Phys., 12, 9817–9854, 2012.
Jeong, G. Y., and Achterberg, E. P.: Chemistry and mineralogy of clay minerals in Asian and Saharan dusts and the implications for iron supply to the oceans, Atmos. Chem. Phys., 14, 12415-12428, 2014.
Jia, X. H., Gu, W. J., Li, Y. J., Cheng, P., Tang, Y. J., Guo, L. Y., Wang, X. M., and Tang, M. J.: Phase transitions and hygroscopic growth of Mg(ClO4)2, NaClO4, and NaClO4·H2O: implications for the stability of aqueous water in hyperarid environments on Mars and on Earth, ACS Earth Space Chem., 2, 159-167, 2018.
Jickells, T. D., An, Z. S., Andersen, K. K., Baker, A. R., Bergametti, G., Brooks, N., Cao, J. J., Boyd, P. W., Duce, R. A., Hunter, K. A., Kawahata, H., Kubilay, N., laRoche, J., Liss, P. S., Mahowald, N., Prospero, J. M., Ridgwell, A. J., Tegen, I., and Torres, R.: Global Iron Connections between Desert Dust, Ocean Biogeochemistry, and Climate, Science, 308, 67-71, 2005.
Jing, B., Wang, Z., Tan, F., Guo, Y. C., Tong, S. R., Wang, W. G., Zhang, Y. H., and Ge, M. F.: Hygroscopic behavior of atmospheric aerosols containing nitrate salts and water-soluble organic acids, Atmos. Chem. Phys., 18, 5115-5127, 2018.
Journet, E., Balkanski, Y., and Harrison, S. P.: A New Data Set of Soil Mineralogy for Dust-cycle Modeling, Atmos. Chem. Phys., 14, 3801-3816, 2014.
Kelly, J. T., and Wexler, A. S.: Thermodynamics of carbonates and hydrates related to heterogeneous reactions involving mineral aerosol, J. Geophys. Res.-Atmos, 110, D11201, doi: 11210.11029/12004jd005583, 2005.
Kelly, J. T., Chuang, C. C., and Wexler, A. S.: Influence of dust composition on cloud droplet formation, Atmos. Environ., 41, 2904-2916, 2007.
Khare, P., Kumar, N., Kumari, K. M., and Srivastava, S. S.: Atmospheric formic and acetic acids: An overview, Rev. Geophys., 37, 227-248, 1999.
Kreidenweis, S. M., and Asa-Awuku, A.: 5.13 - Aerosol Hygroscopicity: Particle Water Content and Its Role in Atmospheric Processes A2 - Holland, Heinrich D, in: Treatise on Geochemistry (Second Edition), edited by: Turekian, K. K., Elsevier, Oxford, 331-361, 2014.
Krueger, B. J., Grassian, V. H., Laskin, A., and Cowin, J. P.: The Transformation of Solid Atmospheric Particles into Liquid Droplets through Heterogeneous Chemistry: Laboratory Insights into the Processing of Calcium Containing Mineral Dust Aerosol in the Troposphere, Geophys. Res. Lett., 30, 1148, doi: 1110.1029/2002gl016563, 2003.

716 Laskin, A., Iedema, M. J., Ichkovich, A., Graber, E. R., Taraniuk, I., and Rudich, Y.: Direct Observation of
717 Completely Processed Calcium Carbonate Dust Particles, Faraday Discuss., 130, 453-468, 2005.
718 Lei, T., Zuend, A., Wang, W. G., Zhang, Y. H., and Ge, M. F.: Hygroscopicity of organic compounds from biomass
719 burning and their influence on the water uptake of mixed organic ammonium sulfate aerosols, Atmos. Chem. Phys.,
720 14, 11165-11183, 2014.
721 Li, H. J., Zhu, T., Zhao, D. F., Zhang, Z. F., and Chen, Z. M.: Kinetics and mechanisms of heterogeneous reaction of
722 NO_2 on $CaCO_3$ surfaces under dry and wet conditions, Atmos. Chem. Phys., 10, 463-474, 2010.
723 Li, W. J., and Shao, L. Y.: Observation of Nitrate Coatings on Atmospheric Mineral Dust Particles, Atmos. Chem.
724 Phys., 9, 1863-1871, 2009.
725 Li, X.-H., Zhao, L.-J., Dong, J.-L., Xiao, H.-S., and Zhang, Y.-H.: Confocal Raman Studies of Mg(NO3)2 Aerosol
726 Particles Deposited on a Quartz Substrate: Supersaturated Structures and Complicated Phase Transitions, J. Phys.
727 Chem. B., 112, 5032-5038, 2008a.
728 Li, X., Dong, J., Xiao, H., Lu, P., Hu, Y., and Zhang, Y.: FTIR-ATR in situ observation on the efflorescence and
729 deliquescence processes of Mg(NO3)2 aerosols, Sci. China-Chem., 51, 128-137, 2008b.
730 Liu, Y., Gibson, E. R., Cain, J. P., Wang, H., Grassian, V. H., and Laskin, A.: Kinetics of heterogeneous reaction of
731 $CaCO_3$ particles with gaseous HNO_3 over a wide range of humidity, J. Phys. Chem. A, 112, 1561-1571, 2008a.
732 Liu, Y. J., Zhu, T., Zhao, D. F., and Zhang, Z. F.: Investigation of the hygroscopic properties of $Ca(NO_3)_2$ and
733 internally mixed $Ca(NO_3)_2/CaCO_3$ particles by micro-Raman spectrometry, Atmos. Chem. Phys., 8, 7205-7215,
734 2008b.
735 Ma, Q. X., Liu, Y. C., Liu, C., and He, H.: Heterogeneous Reaction of Acetic Acid on MgO, α-Al_2O_3, and $CaCO_3$
736 and the Effect on the Hygroscopic Behavior of These Particles, Phys. Chem. Chem. Phys., 14, 8403-8409, 2012.
737 Mahowald, N., Ward, D. S., Kloster, S., Flanner, M. G., Heald, C. L., Heavens, N. G., Hess, P. G., Lamarque, J.-F.,
738 and Chuang, P. Y.: Aerosol Impacts on Climate and Biogeochemistry, Annu. Rev. Environ. Resour., 36, 45-74,
739 2011.
740 Mahowald, N. M., Engelstaedter, S., Luo, C., Sealy, A., Artaxo, P., Benitez-Nelson, C., Bonnet, S., Chen, Y.,
741 Chuang, P. Y., Cohen, D. D., Dulac, F., Herut, B., Johansen, A. M., Kubilay, N., Losno, R., Maenhaut, W., Paytan,
742 A., Prospero, J. M., Shank, L. M., and Siefert, R. L.: Atmospheric Iron Deposition: Global Distribution, Variability,
743 and Human Perturbations, Ann. Rev. Mar. Sci., 1, 245-278, 2009.
744 Massoli, P., Lambe, A. T., Ahern, A. T., Williams, L. R., Ehn, M., Mikkila, J., Canagaratna, M. R., Brune, W. H.,
745 Onasch, T. B., Jayne, J. T., Petaja, T., Kulmala, M., Laaksonen, A., Kolb, C. E., Davidovits, P., and Worsnop, D. R.:
746 Relationship between aerosol oxidation level and hygroscopic properties of laboratory generated secondary organic
747 aerosol (SOA) particles, Geophys. Res. Lett., 37, L24801, DOI: 24810.21029/22010GL045258, 2010.
748 Nickovic, S., Vukovic, A., Vujadinovic, M., Djurdjevic, V., and Pejanovic, G.: Technical Note: High-resolution
749 mineralogical database of dust-productive soils for atmospheric dust modeling, Atmos. Chem. Phys., 12, 845-855,
750 2012.
751 Pan, X., Uno, I., Wang, Z., Nishizawa, T., Sugimoto, N., Yamamoto, S., Kobayashi, H., Sun, Y., Fu, P., Tang, X.,
752 and Wang, Z.: Real-time observational evidence of changing Asian dust morphology with the mixing of heavy
753 anthropogenic pollution, Sci. Rep., 7, 335, doi: 310.1038/s41598-41017-00444-w, 2017.
754 Pang, S. F., Wu, C. Q., Zhang, Q. N., and Zhang, Y. H.: The structural evolution of magnesium acetate complex in
755 aerosols by FTIR-ATR spectra, J. Mol. Struct., 1087, 46-50, 2015.
756 Park, K., Kim, J. S., and Miller, A. L.: A study on effects of size and structure on hygroscopicity of nanoparticles
757 using a tandem differential mobility analyzer and TEM, J. Nanopart. Res., 11, 175-183, 2009.
758 Peng, C., Jing, B., Guo, Y. C., Zhang, Y. H., and Ge, M. F.: Hygroscopic Behavior of Multicomponent Aerosols
759 Involving NaCl and Dicarboxylic Acids, J. Phys. Chem. A, 120, 1029-1038, 2016.
760 Petters, M. D., and Kreidenweis, S. M.: A single parameter representation of hygroscopic growth and cloud
761 condensation nucleus activity, Atmos. Chem. Phys., 7, 1961-1971, 2007.
762 Petters, M. D., and Kreidenweis, S. M.: A single parameter representation of hygroscopic growth and cloud
763 condensation nucleus activity-Part 2: Including solubility, Atmos. Chem. Phys., 8, 6273-6279, 2008.
764 Prenni, A. J., Petters, M. D., Kreidenweis, S. M., DeMott, P. J., and Ziemann, P. J.: Cloud droplet activation of
765 secondary organic aerosol, J. Geophys. Res.-Atmos., 112, D10223, DOI: 10210.11029/12006JD007963, 2007.
766 Prince, A. P., Kleiber, P. D., Grassian, V. H., and Young, M. A.: Reactive Uptake of Acetic Acid on Calcite and
767 Nitric Acid Reacted Calcite Aerosol in an Environmental Reaction Chamber, Phys. Chem. Chem. Phys., 10, 142-
768 152, 2008.
769 Rard, J. A., Habenschuss, A., and Spedding, F. H.: A review of the osmotic coefficients of aqueous calcium chloride
770 at 25 °C, J. Chem. Eng. Dara, 22, 180-186, 1977.

771 Rard, J. A., and Miller, D. G.: Isopiestic determination of the osmotic and activity coefficients of aqueous
772 magnesium chloride solutions at 25 °C, J. Chem. Eng. Dara, 26, 38-43, 1981.
773 Rard, J. A., Wijesinghe, A. M., and Wolery, T. J.: Review of the thermodynamic properties of Mg(NO3)2(aq) and
774 their representation with the standard and extended ion-interaction (Pitzer) models at 298.15 K, J. Chem. Eng. Data,
775 49, 1127-1140, 2004.
776 Ridley, D. A., Heald, C. L., Kok, J. F., and Zhao, C.: An observationally constrained estimate of global dust aerosol
777 optical depth, Atmos. Chem. Phys., 16, 15097-15117, 2016.
778 Robinson, R. A., and Stokes, R. H.: Electrolyte Solutions (Second Revised Edition), Butterworths, London, UK,
779 1959.
780 Romanias, M. N., El Zein, A., and Bedjanian, Y.: Heterogeneous Interaction of H_2O_2 with TiO_2 Surface under Dark
781 and UV Light Irradiation Conditions, J. Phys. Chem. A, 116, 8191-8200, 2012.
782 Romanias, M. N., Zeineddine, M. N., Gaudion, V., Lun, X., Thevenet, F., and Riffault, V.: Heterogeneous
783 Interaction of Isopropanol with Natural Gobi Dust, Environ. Sci. Technol., 50, 11714-11722, 2016.
784 Santschi, C., and Rossi, M. J.: Uptake of CO_2, SO_2, HNO_3 and HCl on calcite ($CaCO_3$) at 300 K: Mechanism and
785 the role of adsorbed water, J. Phys. Chem. A, 110, 6789-6802, 2006.
786 Scanza, R. A., Mahowald, N., Ghan, S., Zender, C. S., Kok, J. F., Liu, X., Zhang, Y., and Albani, S.: Modeling Dust
787 as Component Minerals in the Community Atmosphere Model: Development of Framework and Impact on
788 Radiative Forcing, Atmos. Chem. Phys., 15, 537-561, 2015.
789 Seinfeld, J. H., and Pandis, S. N.: Atmospheric Chemistry and Physics: From Air Pollution to Climate Change,
790 Wiley Interscience, New York, 2006.
791 Shi, Z., Zhang, D., Hayashi, M., Ogata, H., Ji, H., and Fujiie, W.: Influences of sulfate and nitrate on the
792 hygroscopic behaviour of coarse dust particles, Atmos. Environ., 42, 822-827, 2008.
793 Sullivan, R. C., Moore, M. J. K., Petters, M. D., Kreidenweis, S. M., Roberts, G. C., and Prather, K. A.: Effect of
794 Chemical Mixing State on the Hygroscopicity and Cloud Nucleation Properties of Calcium Mineral Dust Particles,
795 Atmos. Chem. Phys., 9, 3303-3316, 2009.
796 Tan, F., Tong, S. R., Jing, B., Hou, S., Liu, Q., Li, K., Zhang, Y., and Ge, M. F.: Heterogeneous reactions of NO2
797 with $CaCO_3$–$(NH_4)_2SO_4$ mixtures at different relative humidities, Atmos. Chem. Phys., 16, 8081-8093, 2016.
798 Tang, I. N., and Fung, K. H.: Hydration and Raman scattering studies of levitated microparticles: $Ba(NO_3)_2$,
799 $Sr(NO_3)_2$, and $Ca(NO_3)_2$, J. Chem. Phys., 106, 1653-1660, 1997.
800 Tang, M. J., Thieser, J., Schuster, G., and Crowley, J. N.: Kinetics and Mechanism of the Heterogeneous Reaction of
801 N_2O_5 with Mineral Dust Particles, Phys. Chem. Chem. Phys., 14, 8551-8561, 2012.
802 Tang, M. J., Whitehead, J., Davidson, N. M., Pope, F. D., Alfarra, M. R., McFiggans, G., and Kalberer, M.: Cloud
803 Condensation Nucleation Activities of Calcium Carbonate and its Atmospheric Ageing Products, Phys. Chem.
804 Chem. Phys., 17, 32194-32203, 2015.
805 Tang, M. J., Cziczo, D. J., and Grassian, V. H.: Interactions of Water with Mineral Dust Aerosol: Water Adsorption,
806 Hygroscopicity, Cloud Condensation and Ice Nucleation, Chem. Rev., 116, 4205–4259, 2016a.
807 Tang, M. J., Larish, W., Fang, Y., Gankanda, A., and Grassian, V. H.: Heterogeneous Reactions of Acetic Acid with
808 Oxide Surfaces: Effects of Mineralogy and Relative Humidity, J. Phys. Chem. A, 120, 5609-5616, 2016b.
809 Tang, M. J., Huang, X., Lu, K. D., Ge, M. F., Li, Y. J., Cheng, P., Zhu, T., Ding, A. J., Zhang, Y. H., Gligorovski,
810 S., Song, W., Ding, X., Bi, X. H., and Wang, X. M.: Heterogeneous reactions of mineral dust aerosol: implications
811 for tropospheric oxidation capacity, Atmos. Chem. Phys., 17, 11727-11777, 2017.
812 Textor, C., Schulz, M., Guibert, S., Kinne, S., Balkanski, Y., Bauer, S., Berntsen, T., Berglen, T., Boucher, O., Chin,
813 M., Dentener, F., Diehl, T., Easter, R., Feichter, H., Fillmore, D., Ghan, S., Ginoux, P., Gong, S., Grini, A.,
814 Hendricks, J., Horowitz, L., Huang, P., Isaksen, I., Iversen, I., Kloster, S., Koch, D., Kirkevåg, A., Kristjansson, J.
815 E., Krol, M., Lauer, A., Lamarque, J. F., Liu, X., Montanaro, V., Myhre, G., Penner, J., Pitari, G., Reddy, S., Seland,
816 Ø., Stier, P., Takemura, T., and Tie, X.: Analysis and Quantification of the Diversities of Aerosol Life Cycles within
817 AeroCom, Atmos. Chem. Phys., 6, 1777-1813, 2006.
818 Tobo, Y., Zhang, D. Z., Nakata, N., Yamada, M., Ogata, H., Hara, K., and Iwasaka, Y.: Hygroscopic mineral dust
819 particles as influenced by chlorine chemistry in the marine atmosphere, Geophys. Res. Lett., 36, L05817, doi:
820 05810.01029/02008gl036883, 2009.
821 Tobo, Y., Zhang, D., Matsuki, A., and Iwasaka, Y.: Asian Dust Particles Converted into Aqueous Droplets under
822 Remote Marine Atmospheric Conditions, Proc. Natl. Acad. Sci. U. S. A., 107, 17905-17910, 2010.
823 Tong, S. R., Wu, L. Y., Ge, M. F., Wang, W. G., and Pu, Z. F.: Heterogeneous Chemistry of Monocarboxylic Acids
824 on α-Al_2O_3 at Different Relative Humidities, Atmos. Chem. Phys., 10, 7561-7574, 2010.
825 Uno, I., Eguchi, K., Yumimoto, K., Takemura, T., Shimizu, A., Uematsu, M., Liu, Z., Wang, Z., Hara, Y., and
826 Sugimoto, N.: Asian Dust Transported One Full Circuit around the Globe, Nature Geosci., 2, 557-560, 2009.

827 Usher, C. R., Michel, A. E., and Grassian, V. H.: Reactions on Mineral Dust, Chem. Rev., 103, 4883-4939, 2003.
828 Vlasenko, A., Sjogren, S., Weingartner, E., Stemmler, K., Gaggeler, H. W., and Ammann, M.: Effect of Humidity
829 on Nitric Acid Uptake to Mineral Dust Aerosol Particles, Atmos. Chem. Phys., 6, 2147-2160, 2006.
830 Wang, L. Y., Zhang, Y. H., and Zhao, L. J.: Raman spectroscopic studies on single supersaturated droplets of
831 sodium and magnesium acetate, J. Phys. Chem. A, 109, 609-614, 2005.
832 Wex, H., Petters, M. D., Carrico, C. M., Hallbauer, E., Massling, A., McMeeking, G. R., Poulain, L., Wu, Z.,
833 Kreidenweis, S. M., and Stratmann, F.: Towards closing the gap between hygroscopic growth and activation for
834 secondary organic aerosol: Part 1 – Evidence from measurements, Atmos. Chem. Phys., 9, 3987-3997, 2009.
835 Zeng, G., Kelley, J., Kish, J. D., and Liu, Y.: Temperature-Dependent Deliquescent and Efflorescent Properties of
836 Methanesulfonate Sodium Studied by ATR-FTIR Spectroscopy, J. Phys. Chem. A, 118, 583-591, 2014.
837 Zhang, Y., Mahowald, N., Scanza, R. A., Journet, E., Desboeufs, K., Albani, S., Kok, J. F., Zhuang, G., Chen, Y.,
838 Cohen, D. D., Paytan, A., Patey, M. D., Achterberg, E. P., Engelbrecht, J. P., and Fomba, K. W.: Modeling the
839 global emission, transport and deposition of trace elements associated with mineral dust, Biogeosciences, 12, 5771-
840 5792, 2015.
841 Zhang, Y. H., Choi, M. Y., and Chan, C. K.: Relating hygroscopic properties of magnesium nitrate to the formation
842 of contact ion pairs, J. Phys. Chem. A, 108, 1712-1718, 2004.
843 Zieger, P., Vaisanen, O., Corbin, J. C., Partridge, D. G., Bastelberger, S., Mousavi-Fard, M., Rosati, B., Gysel, M.,
844 Krieger, U. K., Leck, C., Nenes, A., Riipinen, I., Virtanen, A., and Salter, M. E.: Revising the hygroscopicity of
845 inorganic sea salt particles, Nature Communications, 8, 10.1038/ncomms15883, 2017.
846